Reply to the reviewers

"Conceptual Model to Simulate Long-term Soil Organic Carbon and Ground Ice Budget with Permafrost and Ice Sheets (SOC-ICE-v1.0)" by Kazuyuki Saito et al. in GMDD.

Reviewer #1

General comments:

The authors present a very timely and necessary modelling framework for assessing the spatial distribution of soil organic carbon (SOC) and ground ice (ICE) across the circumpolar permafrost region between the 50th and 70th latitudes. Moreover, the presented SOC-ICE-v1.0 model can be used to produce maps of these distributions at any time point during the last 125,000 years. This is obviously an ambitious task to initiate with, but the authors accomplish in providing modelling tools that have potential to inform about the history and future of permafrost-affected soils. In their recent manuscripts and published works the authors have already assessed future developments and published snapshot maps using outputs from SOC-ICE-v1.0.

Despite the simplified consideration of some relevant factors for SOC and ICE dynamics (very coarse representation of soil properties, only one ice core to force past circumpolar climate deviations), the models show promising performance in reconstructing SOC and ICE histories. What I find impressive is the model's ability to account for the role of continental ice sheets and changing sea level in the reconstructed time series for SOC and ICE. The manuscript is well written. Results are well presented and likely reproducible, although some of the performed pre-examinations are mentioned in a cursory manner.

Concerning the results, the time series over the last 125 ka appear mostly realistic, although the lack of validation data especially for ground-ice accumulation history hinders model evaluations. Despite the comparisons using observations from 8 locations across circumpolar north, I remain rather uninformed about the model's capability to reliably produce the actual spatial SOC and ICE variability. The authors state that the modelled SOC and ICE foremostly paint a picture of relative contents, that is, in relation to other grid cells across the study area and not absolute in situ contents. Rather coarse spatial analysis resolution and very coarse representation of soil properties additionally reduce the model's potential to address the local to regional consequences of organic carbon cycling to the atmospheric GHG or ground subsidence due to ground ice melt. Nevertheless, I consider that at the present SOC-ICE-v1.0 constitutes a fair step towards these goals.

I applaud the authors for their explicit explanations of the performed parameterisations. However, coming from a different modelling tradition, I have recognized and pointed out several places where I believe the methods would benefit from further clarification. Moreover, I have several specific comments and suggestions for the authors to consider before consideration of publication in GMD.

> We thank the reviewer for their sound and detailed review containing informative and constructive comments and suggestions. We have addressed each of these comments and suggestions in a point-to-point manner.
>
> Regarding the actual spatial SOC and ICE variability that the model can produce, we have explicitly demonstrated those reported by Saito et al. (2020, PEPS) for the present-day condition. Further, we have added Figure 10 containing sample snapshot maps for the LGM and mid-Holocene to the revised manuscript to

illustrate the spatial distribution and temporal variability under different climate conditions.

Specific comments:

lines 30-34: As ground ice is the other studied property, I would suggest adding a very brief note on what consequences its melt may have.

We added an explanation of the possible consequences of ground ice melt. (ll. 37–39)

lines 39-40: While yedoma is a prominent type of ice-rich permafrost, all ice-rich permafrost is not exclusively yedoma but other types of ice-rich permafrost occur.

We deleted the word “yedoma” to clarify the sentence. (ll. 45–47)

line 42: I would suggest avoiding the term “buried ice” in the context of ice wedges, as buried ice typically refers to ice accumulated on the ground surface (e.g. glacier, lake, river or sea ice) and later buried by sediments. See, e.g., Permafrost Subcommittee: 1988, Glossary of permafrost and related ground-ice terms, Associate Committee on Geotechnical Research, National Research Council of Canada, Ottawa, Technical Memorandum No. 142, 156 pp.

We deleted the word “buried” in response to the reviewer’s comment, which we agree with. (l. 48)

line 51: Please elaborate. What is "the aerial extent of ice-rich permafrost"?

We modified the sentence to clarify it: “Although the spatial extent of the areas underlain by ice-rich permafrost with high soil carbon contents is limited, the impact of its degradation can reach wider areas globally.” (ll. 57–59)

I wonder if the whole introduction part would read more clearly if the descriptions of SOC accumulation history and research tradition (around the lines 71-84) would be embedded in section 1, and if section 1.1 would then solely focus on general descriptions of the model? Moreover, I am sure that the authors have become aware of a very recent study by Hugelius et al. (2020 PNAS), which appears to have provided notable advances in mapping the circumpolar C distribution. Consider updating parts of the review of current knowledge at lines 57-64 with the information provided therein.

Hugelius et al. (2020) Large stocks of peatland carbon and nitrogen are vulnerable to permafrost thaw. PNAS 117 (34) 20438-20446

We thank the reviewer for providing new information. We moved the descriptions of SOC accumulation history and research tradition to section 1 and updated the description of the circumpolar C distribution mapping using the new information. (ll. 69–74)

lines 90-93: The authors say that they incorporated a key parameter that represents temporal and spatial variations in climatic and topo-geographic conditions. This is related to the whole issue of external, or allogenic, factors, which are referred to in a bit inconsistent way by using terms, such as “climatic or environmental conditioning” (lines 517-518), “climatic, topographic and/or land composition” (399-400) or “climate, hydrology and topography” (77). I wonder if it

would be possible to more explicitly describe what this parameter represents in this study. As far as I understand only continentality (distance to the closest ocean body) and cover ratios of land, water, ice sheet and its thickness were specifically parameterized. DEM-based topographic conditions were only used in the authors' recently published paper (Saito et al. 2020 Progress in Earth and Planetary Science) to downscale the outputs of here presented model.

In addition to direct climate control by temperature and precipitation, a key parameter τ, the value of which reflects the climatic conditions (namely, freeze/thaw, a large value for frozen environment), soil condition (small values for coarse-grain soil), and topo-geographic condition (small values for steep, or well-drained areas) was introduced to represent temporal and spatial variations in climatic and topo-geographic conditions. The continentality (distance to the closest ocean body) and cover ratios of land, water, and ice sheet and its thickness are meant to constitute the boundary conditions for the simulations but are not parameters.

We realize that our explanation of the functionality of the key parameter, τ, in section 2.2.2 (ll. 227–228 in the original manuscript) was not clear enough. We, thus, revised the following relevant sentences to clarify our intended meaning:

"We also incorporated a key parameter, τ, that represented temporal and spatial variations in climatic and topo-geographic conditions (e.g. terrain curvatures, specific catchment areas, continentality, geomorphology, landscape, and fluvial conditions) to evaluate impacts on soil carbon evolution induced by these external factors, which we have discussed in section 2.2.2." (ll. 101–104)

"We also incorporated a key parameter, τ, that represented temporal and spatial variations in climatic and topo-geographic conditions (e.g. terrain curvatures, specific catchment areas, continentality, geomorphology, landscape, and fluvial conditions) to evaluate impacts on soil carbon evolution induced by these external factors, which we have discussed in section 2.2.2." in section 1.1.

"This is the key parameter for the examination of climate and topo-geographic controls on soil carbon evolution, and we set the values of τ in this study in a geometric series at 4, 20, 100, and 500 yr, adhering to considerations" (section 2.2.2).

line 91: What curvatures? Terrain?

Yes, we meant terrain curvatures and have revised the term accordingly. (l. 102)

line 142: Can the authors very briefly clarify what they mean by stating that the Mosaic model outputs showed the best settings and results for regions north of 50_? No detailed explanations of the preliminary analyses are needed but please elaborate "settings and results".

We added a brief explanation to clarify our focus during the selection of model outputs: "After a preliminary analysis of the hydrological outputs of the four models (Noah, CLM, VIC, and Mosaic models), we selected the Mosaic model outputs because they yielded optimum results for cold regions north of 50 °N with respect to evaporation and runoff response to different soil types in the examined range of temperature, -30 ℃ to 15 ℃" (ll. 151–153)

lines 183-184: Does altitude data here refer to the thickness of an ice sheet or a digital elevation model? Related to this,

clarifications on the used elevation data (if any) is needed. In the reference list the authors have Amante and Eakins (2009) and Tarboton (1989) related to DEM's but they are not cited in the text. Having read the authors' recent paper (Saito et al. 2020 Progress in Earth and Planetary Science) where they produced maps using SOC-ICE-v1.0, it appears that the related DEM was therein used to downscale model outputs.

The "altitude data" (we changed it to "orography condition" in line with the CMIP5/PMIP3 convention) refers to the elevation of the grid points used in each of the GCMs from the mean sea level. (l. 199)

We deleted two citations, Amante and Eakins (2009) and Tarboton (1989), from the manuscript as these DEM-related data were used by Saito et al. (2020, PEPS) and not in this study as the reviewer correctly pointed out.

Figure 3: Consider adding an explanation of the presented subsurface layers. Does the brown box refer to permafrost or impenetrable surface in general?

We added an explanation for the subsurface box, which, similar to a bucket-type model, does not resolve the vertical profile, but only retains the composition ratio.

lines 295-297: Could this examination of "overall goodness of the reproduced time series" benefit from an elaboration or a reference?

We modified the sentence to clarify as "We examined the SOC time series calculated using the forcing data obtained from the CMIP5/PMIP3 models for the period (the Last Millennium and the historical runs), with respect to the mean values, temporal variability and smooth connectivity to the historical period, to select the IPSL simulation results." (ll. 306–308)

Figure 4: The caption suggests that results from litter fall diagnosis are shown but they are missing.

As the litter fall diagnosis was illustrated in Figure 6 (left-most column), the associated words were deleted from this figure's caption.

lines 315-318: Supplementary Fig. 2 could benefit from a more detailed caption (naming the 6 models, explaining the symbols).

We added an explanation for the 6 models and the symbol in Supplementary Fig. 2.

Figure 5: Please align the panels to the same level and maybe label latitudes and longitudes.

We revised the panel for alignment and added the latitude and longitude labels.

lines 337-338, I had problems understanding this sentence. In the Discussion (lines 527-532), the authors provided a clear account on how the initial values for the spin-up were derived. I recommend presenting that piece of text in the Methods, so the spin-up is easier to understand.

We reorganized the structure of the manuscript by moving both sentences that explain the initial values in the original "Discussion" section (ll. 527–532 in the original) along with the aforementioned sentence to a new

subsection, “2.3.3 Initial values and spin-up” to explain our selection of the initial values and the spin-up procedure used in this study.

Please also consider elaborating what “5000 yr” means in this context – point in time or a period for which the model was spun up? Spin-up may also not be familiar for all readers, so maybe open that a little.

We revised the sentence to clarify our intended meaning: “Before full integration, the model was spun up (or equilibrated) for a certain period of years to attain an internal balance in the SOC, soil moisture and ICE budget with the forcing. We integrated the model for 5000 years for spin-up with the constant forcing and perpetual boundary data taken from the 125 ka condition, starting from the uniform initial values of 25.0 kgC m^{-2} of SOC and 500 mm of soil moisture at all grid points to reach an equilibrated state.” (ll. 341–344)

lines 368-369: Check language, some words seem to be missing from where the permafrost zone for Kevo site is mentioned.

We revised the sentence for clarity. (ll. 356–358)

line 371-372: Please revise the statement/language that Anaktavuk and Yakutsk locate “in areas that include the ice-rich permafrost (Yedoma) region”. Yedoma, or other ice-rich permafrost regions, are not confined to these areas.

We revised the statement as follows: “Anaktuvuk and Yakutsk are obtained from areas where the ice-rich permafrost can be found”. (l. 360)

The results section has some sentences that would be better situated in the Discussion (e.g., lines 397-401, 407-411). Would it make sense to title this section Results and Discussion? The current Discussion is relatively short in comparison to the Results.

In adherence to the reviewers’ advice, we merged sections 3 and 4 under “Results and discussions” section and divided section 3.1 to subsections 3.1.1 to 3.1.3 to improve organizational structure. Further, we revised the sentences throughout the section to clearly distinguish the results, cited values from the references, and discussions.

Chapter 3.2: In this chapter (more precisely, in section 3.2.3.), the authors also examine the simulated results of ice accumulation and dissipation, so it could be mentioned in this preamble (lines 430-436).

We mentioned ground ice simulations as the reviewer suggested. (ll. 445-447)

Chapter 3.2.1: I think that the authors do good job in discussing the possible reasons for the discrepancy between observed and simulated basal age. For example, the used climate data reconstruction from one ice core anticipatedly affects the results as the authors later discuss in 4.2. Related to this, in some point of the manuscript it would be beneficial to provide a brief reasoning behind using only one ice core and why it is suitable in the present purpose.

We revised a paragraph in section 3.3.2 (former 4.2) to state the reasons for using only single-core reconstruction in this study. (ll. 528–534)

lines 472-473: I wonder about the large melting of ground ice during 14-15 ka, given that at least Kevo was under the continental ice sheet at that time. Is the anomalous melting related to glacial dynamics or warming climate, and also around 11 ka when the ice sheet finally retreated from the area? Could the authors say something more precise about past glacial/ground-ice dynamics here in order to assess the reliability of the model as no independent observation-based validation data is available?

> We argue that this apparent synchronous melting in relatively southern areas (i.e. compared to high-latitude Alaska or west Canada) occurred because the reconstructed temperature with the warming peak of the SeaRISE time series (likely for the Bølling-Allerød interstadial) exceeded the melting threshold for those regions. We added the following information regarding the simulated extensive melting of ground ice.
>
> "These apparent synchronous melting in these areas likely resulted from the single-sourced warming peak of the Bølling-Allerød interstadial in the SeaRISE time series (e.g. Fig. 4a-c) and suggests the need of further studies to include local climate variations to the driving data". (ll. 488–490)

lines 501-502: Please revise the sentence. It could be made more readable, e.g. the expression "locality-prone profiles".

> We revised the sentence as follows: "…forcing data should be designed to accommodate information that is more specific to the local history so that the resulting time series and maps can reflect regional diversity and characteristics more adequately". (ll. 543–544)

lines 527-532: Explaining this procedure would have seriously helped to understand the initial forcing values first presented in the beginning of the Results section. I thus suggest relocating this text to the Methods. Please also see my comment for lines 337-338.

> We moved these sentences to the new subsection "2.3.3 Initial values and spin-up" and added an explanation for the spin-up procedure.

line 536: I guess that by "relative" risks the authors here may refer to their earlier statement on how the model results do not necessarily represent the absolute SOC or ICE at a grid cell but rather their amounts relative to other grid cell? However, I think this is not clear in the first sentence of the Conclusion, and thus here "relative" could be removed.

> The overall study objective was to assess the relative contributions of the three pathways to greenhouse gas release by permafrost degradation. However, as it has little relevance in regard to the scope of this manuscript, we deleted the term "relative" throughout the text to improve clarity. (l. 577)

lines 551-552: Do the authors here refer to another study using their model?

> We deleted the sentence as it was not relevant to the context.

Technical corrections:

line 10: Is "relative" relevant or understandable without context?

> The overall study objective was to assess the relative contributions from the three pathways to greenhouse gas

release due to permafrost degradation. However, since it is less relevant concerning the scope of this manuscript, we deleted the term “relative” throughout the text to improve clarity. (l. 11)

line 39: "ice-rich-permafrost" to "ice-rich permafrost"

We have corrected it. (l. 45)

line 54: is “relative” needed?

We deleted this term throughout the text to improve clarity. (l. 61)

line 58: Please correct “Gorham 19991”

We corrected to Gorham (1991). (l. 65, l. 73)

line 114: In the abstract, the authors write "A conceptual and a numerical soil organic carbon–ground ice budget model". Are they separate models or one model as stated here (“The developed conceptual numerical model...”)? Please be consistent throughout the text.

We deleted the term “conceptual” from the title, abstract, and main text to clarify that the model proposed in the paper is a numerical model.

line 142: Rodell and Beaudoing ...., publication year missing.

We added the publication year (2007). (l. 154)

lines 175: “closest ocean, distance from the coast of the closest ocean” Is “closest ocean” redundant?

We removed the first occurrence of “closest ocean” to reduce redundancy. (l. 189)

Table 1: kpice to kice

We have corrected it accordingly.

Table 2. Please consider explaining in the caption what the tau symbol denotes. Ta and Pr could also be explained. What does “Simulated ground ice is in meter” mean in footnote d?

We added an explanation for tau symbol, as well as for the abbreviation Ta and Pr, in the caption and in the footnote. We revised the explanation in the footnote d) for clarity.

line 394: Saito et al. 2020, not in review anymore.

We updated the citation. (l. 409)

line 419: Anaktavuku to Anaktavuk

We checked and corrected the spelling in texts, figures, and tables, following the notations in Iwahana et al. (2016). (l. 360)

line 420: length of the thawed layer?

We changed to “length of the thawing period and depth of the thawed layer”. (l. 435)

lines 454-457: This information (starting from “, and then sorted to...”) is found in the caption for Figure 8, and thus not necessary here.

We deleted the sentences accordingly.

At line 481, could the authors repeat the temporal resolution, i.e., for how long a period the snapshot maps can be compiled.

We mentioned that the temporal resolution is annual (l. 498). Theoretically (i.e. without practical concerns and limitations on storage size), any year during the 125 kyr integration can be compiled to make a snapshot map.

line 482: Saito et al. 2020 now published

We updated the citation. (l. 510)

line 491: There are Yokohata et al. 2020 a and b in the Refences, which one does this cite to? Is it published?

As Yokohata et al. (2020a) is less relevant to our study, we deleted it, and revised Yokohata et al. (2020b) to Yokohata et al. (2020). (l. 518)

line 499: I think the last sentence; “Below is a list...” is not necessary here.

We have deleted the sentence.

line 503: Thence to Hence

We revised the relevant sentences. (ll. 535–537)

line 508: Do the referred timings of initiation refer to the results here, or by Morris et al. 2018?

We revised the sentence to indicate that they were reported by Morris et al. (2018). (ll. 540–542)

line 513: “may improve function” could be clarified/said in a different way

We revised the sentence for clarity. (ll. 548-550)

line 532: I suggest editing; “less than a dozen” to “eight”

We have corrected to “eight”. (l. 573)

At least the following listed refs are not cited in the text:

- Amante and Eakins 2009: removed from the list
- AMAP (SWIPA) 2017: cited in the text (l. 32, l. 39)

- Biasi et al. 2005 (Biasi et al. 2013, however, is cited but not in the references): Biasi et al. (2013) replaced with Biasi et al. (2005) in the text (l. 559-560)

- Bradley 1999: removed from the list

- Tarboton 1989: removed from the list

The following, in turn, not found in the References:

- Yu et al. 2008: corrected to Yu et al. 2009 in the text (l. 468)

- Brown et al. 1998: added in the list

Please check all citations and references. We checked all the citations and references.

Reviewer #2:

General comments:

In the manuscript (MS), Saito et al. developed a numerical soil organic carbon–ground ice budget model (SOC-ICE-v1.0) to compute long-term evolution of soil organic carbon (SOC) and ground ice (ICE). The model was developed for the last 125 thousand years for areas north of 50_N. Based on the authors, the simulated results successfully (i) reproduced temporal changes in northern SOC and ICE, consistent with current knowledge and (ii) captured regional differences in different geographical and climatic characteristics within the circum-Arctic region. Moreover, the authors considered that the resulting circum-Arctic set of simulated time series can be compiled to produce snapshot maps of SOC and ICE distributions for the past and present assessments or future projection simulations. Saito et al. concluded that the model provides substantial information on the temporal evolution and spatial distribution of circum-Arctic soil carbon and ground ice. However, model improvements in terms of, e.g., forcing climate data and choice of initial values are required in the future.

It is evident that the authors have addressed a topical issue, spatiotemporal prediction of soil organic carbon and ground ice across the circumpolar permafrost area. Moreover, the period of time is notable, the last 125 ka years. To my opinion, the topic of the MS fits well to Geoscientific Model Development (GMD). In general, I consider this MS to be relatively concise and well-written. However, I have two major concerns and some suggestions to improve the work.

> We thank the reviewer for the appreciation, and for the questions and comments that helped us in enhancing the scientific as well as expressional contents of the manuscript. We have provided a point-to-point reply to the comments and suggestions below:

First, there seems to be overlap between this MS and Saito et al. (2020) published in Progress in Earth and Planetary Science. Please clarify the novelty and added value of this MS.

> Saito, K., Machiya, H., Iwahana, G., Ohno, H., & Yokohata, T. (2020). Mapping simulated circum-Arctic organic carbon, ground ice, and vulnerability of ice-rich permafrost to degradation. Progress in Earth and Planetary Science, 7(1), 1-15.

> This manuscript aims to describe the detailed constructions of the novel numerical model (Sections 2.2 and 2.3) along with the evaluations of the simulated results (time series) in terms of the spatial variations (Section 3.1) and dynamic behaviours (Section 3.2) in SOC, ICE and soil moisture.
>
> In contrast, Saito et al. (2020, PEPS) aimed to demonstrate the applicability of the simulated results for a specific time, namely the present-day, and downscaled the results with other topographical and hydrological information to produce spatial maps of SOC and ICE with relatively finer horizontal resolution and to evaluate the vulnerability distribution of ice-rich permafrost for the degradation. We agree that these originally-intended differences were weakened during the process of reviewing the PEPS manuscript as we were requested by a reviewer to include a relatively detailed description of the model construct and evaluations on the time series of the forcing and simulated data.

Second, how reliable are the results of SOC and ICE for areas covered by glaciers (e.g. continental ice sheets)? How these results relate to the fact that, for example, the site in northern Europe (Kevo) was covered by continental ice sheet

until ca. 10 ka? The model seems to produce substantial variation in SOC despite the presence of glacier ice cover.

> The value of SOC is initialized (i.e. made to null) and ICE is allowed to change when the overlying ice sheet retreats, as described in section 2.3.2. In the current model, the extents of changes in ice sheets (coverage or retreat) are determined by the ICE-6G_C dataset at the 1° horizontal resolution. Sub-grid-scale changes (e.g. extent of ice sheet shrinking, changes in coastline locations, and submergence/uplift of land within the 1° grid) are only considered through changes in occupancy proportion. As shown in Fig. 6 (second from the right, 6th row), the ice sheet (in yellow) dominantly covered the grid point closest to Kevo until approximately 10 ka; the ground ice started melting and soil water level fluctuated from 10 ka. We agree that the appropriateness of allowing for the accumulation of ground ice under the ice sheet cover condition, as discussed in section 3.1.2 (formerly 3.1), requires further consideration. We appreciate the reviewer for bringing this to our attention.

Specific comments:

Title: Please reassess the use of 'conceptual' in the title. I would see the model as 'numerical' rather than 'conceptual'. In the Abstract (and elsewhere), you use 'a conceptual and a numerical...'. For me a conceptual model differs from a numerical model but here the presented SOC-ICE v1.0 is both. Could you please clarify the motivation for the combination of conceptual and numerical?

> Originally, we aimed to indicate that this study is a numerical realization of a conceptual two-box model. However, as both reviewers suggest, it is very confusing. Thus, we removed the word "conceptual" to improve clarity.

It would be nice to have information on the spatial resolution of the model outputs somewhere in the Abstract. This could be relevant also in the Introduction or in the beginning of the section 2.

> We added information on the spatial resolution (i.e. 1°) of the simulations. (l. 25, l. 93, and l. 126)

Introduction: maybe it would good to include definition of permafrost.

> We obtained the definition of permafrost from the IPA's glossary definition and added it to the introduction (van Everdingen, 1998). (ll. 32–34)

Lines 37-39: You state that '...well-recognized and widely examined using...' but refer only to one paper. Maybe few references more?

> We revised the sentence to "…well-recognized and widely examined using global-scale models including Earth System Models (ESMs) and Global Climate Models (GCMs)", and added three more references. (ll. 42–45)

Lines 46-52: I would present the 'second pathway' and 'third pathway' in reverse order. The third is more significant pathway?

> We agree that the third pathway (or secondary release by decomposition of soil carbon newly exposed by permafrost degradation) is significant than the second pathway (direct release of bubbles trapped in ice). However, the direct release likely occurs earlier than the secondary one. Thus, we retained the original order.

Line 59: Could Hugelius et al. (2020) published in PNAS be relevant here?

Hugelius, G., Loisel, J., Chadburn, S., Jackson, R. B., Jones, M., MacDonald, G., ... & Treat, C. (2020). Large stocks of peatland carbon and nitrogen are vulnerable to permafrost thaw. Proceedings of the National Academy of Sciences.

Thank you for providing this information; we added the citation to the manuscript and revised the paragraph. (ll. 69–74)

Lines 72-74: Need for so many references here?

We selected the references according to their relevance and significance to the context of the study. (ll. 76–77)

Line 177: Why the warm period was set to start at 14 ka? For example, Holocene began ca. 11,5 ka before the present.

We set to start the warm period at 14 ka to include the warm environment under the Bølling-Allerød interstadial and avoided quick reversals afterwards via the Younger Dryas and so on. Observation of the sensitivity of the background climatic conditions will be problematic.

Sections 3.1, 3.2.1 and 3.2.2: I find it problematic to include references in the Result sections (results of this MS can be confused with published ones; look like discussion).

We reorganized the structure of the manuscript (sections 3 and 4 are now combined under one section: "Results and discussions") and revised the sentences to make distinctions between the results of this study, those from related studies, and discussions.

Lines 474-476: Do the literature support the mostly negative balance (accumulation rates) across the permafrost region for the past 12 ka? Please consider this in the Discussion.

We revised this paragraph and elaborated the discussion using reported literature from relevant studies. (ll. 475–480)

Line 480 (also in the Abstract and Conclusion): You highlight the possibility to produce snapshot maps. Please provide some maps as examples in the MS.

We provided sample snapshot maps for the LGM and mid-Holocene with different τ values in Figure 10. Another example of the present-day (year 0 = 1950) is already presented in Figure 5a–d with reference to Saito et al. (2020) (ll. 499–509)

Section 4.2: You focused on soil carbon in this section. How to improve the model outcomes related to ground ice?

We added text on future improvement with respect to hydrology and ice dynamics in this paragraph. (ll. 561–569)

Lines 551-552: The sentence ('One of these...') should be removed (not relevant here).

We agree and have deleted the sentence.

Table 1: In Eg. (4), why there are same figures for sand and clay? Their hydrological properties are different.

It was a typo; the value for clay is 0.03.

Table 2: There is no information for the 'Ta' and 'Pr' in the caption? If these area air temperature and average precipitation, please give information from what period they are? At least, some of the figures seem to be odd for modern annual averages.

We added an explanation for the abbreviation Ta and Pr and the period over which climatology was calculated in the caption and footnote. We checked and corrected some figures for Ta and Pr. However, site names such as Fairbanks and Kevo are labels representing the nearest 1° resolution grid point, at which the Ta and Pr values are obtained in the aggregated climate dataset. In some cases, they may be different. We revised the explanation in the caption to improve clarity.

Technical corrections:

Line 15: You could add 'permanently' (...permanently frozen...)

We added this word to the text. (l. 14)

Line 18: You could add 'ground' (...and ground ice...)

We revised to use the abbreviations (i.e. SOC and ICE) in the abstract.

Line (and elsewhere): Should the references be in chronological (or alphabetical) order?

We corrected the references in chronological order throughout the text.

Lines 58 and 64: Please correct Gorham 19991.

We revised this to Gorham (1991). (l. 65, l. 73)

Line 107: Need to add 'soil' (soil carbon) and 'ground' (ground ice)?

We added the words "soil" (soil carbon) and "ground" (ground ice). (l. 117)

Line 169: Should 'annual mean temperature' be 'MAAT'?

We revised this to "MAAT". (l. 183)

Lines 455-457: I would remove the sentence 'The lowest and highest whiskers of the box-whisker...'. This is good in caption but not needed here.

We deleted this sentence.

All abbreviations in the Figures and Tables should be spelled out in the captions.

We spelt all the abbreviations in the Figures and Tables.

~~Conceptual~~Numerical Model to Simulate Long-term Soil Organic Carbon and Ground Ice Budget with Permafrost and Ice Sheets (SOC-ICE-~~01~~v1.0)

Kazuyuki Saito[1], Hirokazu Machiya[1], Go Iwahana[2], Tokuta Yokohata[3], Hiroshi Ohno[4]

[1]Research Center for Environmental Modeling and Application, JAMSTEC, Yokohama, 236-0001, Japan
[2]International Arctic Research Center, University of Alaska Fairbanks, Fairbanks, 99775, USA
[3]National Institute for Environment Studies, Tsukuba, 305-0053, Japan
[4]Kitami Institute of Technology, Kitami, 090-8507, Japan

Correspondence to: Kazuyuki Saito (ksaito@jamstec.go.jp)

Abstract. ~~Degradation~~The degradation of permafrost is a large source of uncertainty in understanding the behaviour ~~of~~ and projecting the future impacts of Earth's climate system ~~and in projecting future impacts of climate change. In assessing and projecting the relative risks and impacts of permafrost degradation, the~~. The spatial ~~distribution~~distributions of soil organic carbon (SOC) and ground ice (ICE) ~~provides~~provide essential information ~~for~~ for the assessment and projection of risks and impacts of permafrost degradation. However, uncertainties ~~in~~ regarding the geographical distribution and ~~in the~~ estimated range of the total amount of stored carbon and ice are still ~~large. A conceptual and a~~substantial. A numerical soil organic carbon–ground ice budget model, SOC-ICE-~~01, was developed, which~~v1.0, that considers essential aspects of carbon and hydrological processes ~~for~~in above ground and subsurface environments and permanently frozen ground (permafrost) and land cover changes (ice sheets and coastlines~~),~~) was developed to calculate the long-term evolution of ~~soil organic carbon (~~local SOC~~)~~ and ~~ground ice (~~ICE~~).~~. The model was integrated ~~for~~to cover the last 125 thousand years~~,~~: from the Last Interglacial ~~until today~~to date for areas north of 50°N at 1° resolution, to simulate the balance between accumulation and dissipation of ~~carbon~~SOC and ~~ice~~ICE. Model performance was compared with observation-based data and evaluated to assess allogenic (external) impacts on soil carbon dynamics in the circum-Arctic region on a glacial-interglacial time scale. Despite the limitation of forcing climate data being constructed on the basis of a single Greenland ice core dataset, the simulated results successfully reproduced temporal changes in northern SOC and ICE, ~~consistent~~in consistence with current knowledge. The simulation also captured regional differences in different geographical and climatic characteristics within the circum-Arctic region. The model quantitatively demonstrated allogenic controls on soil carbon evolution ~~by~~represented by a key parameter that reflects climatological and topo-geographical factors. The resulting circum-Arctic set of simulated time series can be compiled to produce snapshot maps of SOC and ICE distributions for past and present assessments or future projection simulations. Examples of 1° resolution maps for the Last Glacial Maximum and mid-Holocene periods were provided. Despite a simple modelling framework, SOC-ICE-~~01~~v1.0 provided substantial information on the temporal evolution and spatial distribution of circum-Arctic ~~soil carbon~~SOC and ~~ground ice~~ICE. Model improvements in terms of

forcing climate data, improvement of ~~soil carbon~~SOC and ICE dynamics, and choice of initial values are, however, required for future research.

1 Introduction

Degradation of permafrost is a large source of uncertainty in understanding the behaviour ~~of Earth's climate system~~ and ~~in~~ projecting the future impacts of Earth's climate ~~change~~system (AMAP (SWIPA) 2011, ~~2017,~~ IPCC, 2013, AMAP (SWIPA) 2017,). Permafrost is defined as ground (soil or rock and included ice and organic material) that remains at or below 0 °C for at least two consecutive years (van Everdingen 1998). Understanding the additional loss of soil carbon and release of greenhouse gases (GHGs) induced by permafrost degradation is important. This is because the impact is experienced far outside the cryosphere (Plaza et al. 2019) and this phenomenon may accelerate global warming through positive feedback (Schuur et al. 2011, Schaefer et al. 2014, Dean et al. ~~2018a).~~ 2018a, Hugelius et al. 2020). The melting of ground ice, another important aspect of permafrost degradation, may cause surface subsidence (thermokarst) and terrain instability, leading to coastal retreat, slope collapses, damages on social infrastructures, and changes in hydrology and ecology in the Arctic region (Jorgenson et al. 2015, AMAP (SWIPA) 2017)

Three pathways can be considered for additional GHG release ~~to~~into the atmosphere from ~~a~~ warming permafrost. The first occurs in ~~wide~~vast areas through slow and mostly reversible warming and deepening of the active layer (upper soil layer that thaws and freezes seasonally) with a longer thawing period, primarily induced by thermal conduction. This pathway has already been well-recognized and widely examined using global-scale models including Earth System Models (ESMs) and Global Climate Models (GCMs) (Koven et al. ~~2015).~~2015, Schneider von Deimling et al. 2015, McGuire et al. 2016, Yokohata et al. 2020). The second and third pathways are related to the degradation of ice-rich~~-~~ permafrost. Ice-rich permafrost ~~(often called *Yedoma*)~~ is found predominantly in Siberia and Alaska (Kanevskiy et al. 2011, 2013, Murton et al. 2015, Jorgenson et al. 2015, Strauss et al. 2016) and contains massive ~~ground ice~~amounts of ICE (60% to 90% ~~by~~in volume) and carbon-rich sediments. Ice wedge formation is the process responsible for producing the huge amount of ~~buried~~ ice, over a long time in a very cold environment (French 2007, Kanevskiy et al. 2011, 2014, Murton et al. 2015, Jorgenson et al. 2015, Strauss et al. 2016). Soil organic content (SOC) also accumulates ~~alongside~~simultaneously over a long time. Once the ground ice melts ~~by~~owing to triggers such as lateral erosion on coasts and riversides or wildfires, GHGs trapped in ice are readily and directly released to the atmosphere (Brouchkov and Fukuda 2002). This constitutes the second pathway (direct release). In addition, old immobile ~~soil organic carbon (~~SOC~~),~~, stored frozen in permafrost, is exposed to the surface for decomposition, producing new GHGs. This 'secondary release by ice-rich permafrost degradation' constitutes the third pathway (Strauss et al. 2016, Walter-Anthony et al. 2018, Plaza et al. 2019, Turetsky et al. 2020). Depending on the environment where decomposition occurs (i.e~~.~~, dry and aerobic, or wet and anaerobic), the resulting gas differs. Carbon dioxide (CO_2) is mostly produced ~~mostly~~ in the former case, while methane (CH_4) is ~~more likely~~often produced in the latter case (Schuur et al. 2011, Dean et al. 2018b). ~~The aerial~~Although the spatial extent of the areas underlain by ice-rich

permafrost with high soil carbon contents is limited ~~but its~~, the impact of its degradation can ~~be global~~reach wider areas globally (Murton et al. 2015, Strauss et al. 2016, Turetsky et al. 2020).

In assessing and projecting the ~~relative~~ risks and impacts of permafrost degradation among the three pathways, the spatial distribution of SOC and ground ice (ICE) provides essential information. The target area is the circum-Arctic because of the high areal occupancy of permafrost and accumulation of SOC and ICE (Murton et al. 2015, Strauss et al. 2016, Brown et al. ~~1997~~1998). The amount of carbon accumulated in northern soils, including peatlands, accounts for a substantial part of the global soil carbon budget (Gorham ~~19991~~1991, Yu et al. 2010, Hugelius et al. 2014, Nichols and Peteet 2019). Currently available maps and data for near-surface SOC (Hugelius et al. 2014, Olefeldt et al. ~~2015~~2016) and ICE content (Brown et al. ~~1997~~1998) in the circum-Arctic region are compiled from contemporary samples or cores through interpolation or extrapolation using other topo-geographical and geological information. However, the number of samples and cores is often limited or spatially biased mainly due ~~mostly~~ to the remote and harsh environment (e.g.~~,~~, cold, altitude, lack of access). ~~Thus~~Recently, Hugelius et al. (2020) updated the circum-Arctic maps of carbon and nitrogen storages by employing machine-learning techniques applied to a large number (more than 7,000) of peat core samples and offered additional insight into the stock distribution and their vulnerability in the northern permafrost region. Yet, uncertainties ~~in~~ regarding the geographical distribution ~~(Hugelius et al. 2014) and in the~~and estimated range of the total amount of stored carbon ~~are still large~~ continue to be arguable (Gorham ~~19991~~1991, Yu et al. 2010, Nichols and Peteet 2019, Hugelius et al. 2020).

~~**1.1 Carbon and ice accumulation model**~~

~~In our research, we adopted a different approach to estimate the spatial distribution and amount of SOC and ICE. We developed a conceptual numerical model of two boxes (one for above ground and one for the subsurface) to compute the evolution of SOC and ICE, at a timescale long enough to reproduce present-day conditions by covering more than one cycle of development (i.e., initiation, formation, development, maturation, and decay).~~

Northern soil carbon (mostly but not entirely in peatlands) was formed and developed during the postglacial period after the Last Glacial Maximum (LGM, around 21 thousand years before present, or 21 ka) (~~Smith et al. 2004,~~ McDonald et al. 2006, Yu et al. ~~2009,~~ 2010~~, Beilman et al. 2009, Klein et al. 2013, Xing et al. 2015, Charman et al. 2015~~, Loisel et al. 2017, Morris et al. 2018, Nichols and Peteet 2019). Soil carbon dynamics are determined by the balance between inputs (~~how much~~amount of carbon that is deposited ~~and enters~~ into the soil) and outputs (~~how much~~amount of carbon that is lost by decomposition or transfer from the soil) of carbon in soil layers, and are controlled by autogenic (internal conditions specific to the ecosystems) and allogenic (external conditions such as climate, hydrology, and topography) factors (Belyea and Baird 2006, Lund et al. 2010, Klein et al. 2013, Charman et al. 2015, Loisel et al. 2017, Jassey and Signarbieux 2019). Owing to temporal changes and geographic characteristics in these factors, carbon accumulation profiles, such as initiation periods or basal ages of accumulations (Smith et al. 2004, McDonald et al. 2006, Yu et al. 2009) and accumulation rates (Harden et al.

1992; Nichols and Peteet 2019) ~~differ from region~~vary according to the region; some of the regions studied previously include Siberia (Smith et al. 2004; Beilman et al. 2009), Alaska (Klein et al. 2013), Northeast China (Xing et al. 2015), Canada (Charman et al. 2015), the circum-Arctic region (Yu et al. 2009, 2010, Hugelius et al. 2014, Olefeldt et al. ~~2015~~2016, Nichols and Peteet 2019, Hugelius et al. 2020), the Southern Hemisphere (Patagonia: Loisel and Yu 2013), and around the globe (Morris et al. 2018). Many researchers have modelled soil carbon dynamics with varying complexities and for various targets at different spatial and temporal scales (Jenny et al. 1949, Ingram 1978, Clymo 1984, Harden et al. 1992, Yu et al. 2003, Belyea and Baird 2006, Morris et al. 2018).

1.1 Carbon and ice accumulation model

In ~~this study~~our research, we adopted a diachronic approach, different from synchronic core sample aggregations, to estimate the spatial distribution and amount of SOC and ICE at 1° resolution. We developed a numerical model, consisting of two boxes (one for above ground and one for the subsurface), to compute the evolution of SOC and ICE at a time scale that was long enough to reproduce present-day conditions by covering more than one cycle of development (i.e. initiation, formation, development, maturation, and decay).

We employed a simple ~~conceptual~~idealistic setting to evaluate long-term evolution of generic soil carbon. The ~~analysis~~target was not necessarily limited to peatlands~~; further~~. Further, it was based on Clymo-type growth modelling (Clymo 1984, 1992), ~~in which~~wherein slow carbon processes occurring in the 'catotelm' (the layer underlying the upper 'acrotelm' of faster carbon processes) were implemented (Clymo 1984, 1992, Yu et al. 2003, Belyea and Baird 2006). We also incorporated a key parameter, τ, that ~~represents~~represented temporal and spatial variations in climatic and topo-geographic conditions (e.g.~~,~~, terrain curvatures, specific catchment areas, continentality, geomorphology, landscape, and fluvial conditions) to evaluate impacts on soil carbon evolution induced by these external factors~~.~~

~~As for~~, which we have discussed in section 2.2.2. With respect to hydrology, we adopted a one-box budget for liquid and solid water dynamics, which is much simpler than in land surface models employed in coupled system models (e.g.~~,~~ Rodell et al. 2004) but more flexible to handle ground ice storage. Soil column layering of the conventional land surface scheme with fixed thickness does not properly represent ~~such massive ground ice as in *Yedoma*. Since~~excess ICE. As most of the currently observable active periglacial features of permafrost-related processes, especially massive ~~ground ice~~ICE in ice-rich permafrost, formed between the Last Glacial Period and the Holocene (Lunardini 1995, French 2007, Kanevskiy et al. 2011, 2013, Murton et al. 2015, Willeit and Ganopolski 2015, Strauss et al. 2016), the integration period was determined to cover the last 125 thousand years since the Last Interglacial (Kukla et al. 2002), which sufficiently covers the carbon accumulation cycle (Morris et al. 2018, Loisel et al. 2017, Yu 2011, McDonald et al. 2006).

Climate data for the circum-Arctic region (north of 50°N) were reconstructed for the integration period to ~~force~~drive the model. The resulting model outputs can be compiled to produce contemporary spatial maps of estimated SOC and ICE storage for any time ~~slice~~period, including the present day. Such a model is also expected to quantitatively demonstrate the long-term subsurface dynamics of soil carbon and ground ice under varying climatic and environmental conditions, reproduce the long-time evolution of carbon and ice accumulation and decomposition (or dissipation), and provide new insights into ~~understanding~~ the effect of external factors on respective dynamics.

The development of the model and the data used for determining model parameters or driving the model are described in Section 2. Section 3 presents the results~~, followed by discussion~~ and discussions, including future research ideas ~~in Section 4~~.

2 Methods

The developed ~~conceptual~~ numerical model describes essential aspects of subsurface carbon dynamics and hydrological processes, to calculate the balance of SOC and ICE. The model simulates SOC and ICE accumulation (or dissipation) history in the circum-Arctic region on a glacial-interglacial time scale~~.~~ at 1° resolution. Implemented carbon dynamics processes include the supply of carbon from the surface and loss by decomposition under the ground. Implemented hydrological processes include net infiltration (i.e~~.~~, precipitation minus evapotranspiration and surface runoff) from the surface, base runoff, and phase changes between solid and liquid states. The model is forced annually by climate variables, namely temperature and precipitation. Major parameters used for carbon and hydrological processes were determined or parameterized using the climatic datasets and geographical information described in Section 2.1. In this study, driving data were reconstructed from Greenland ice core data and applied to the circum-Arctic region to calculate the evolution of SOC, soil moisture, and ICE.

2.1 Datasets used to develop and evaluate the model

The datasets used to determine the parameters of the model included several reanalysis data for the historical period (since 1850), simulation outputs from global-scale climate models for preceding periods, specifically from the Climate Model Intercomparison Project: Phase 5 (CMIP5, Taylor et al. 2012) and the Paleoclimate Model Intercomparison Project: Initiative 3 (PMIP3, Braconnot et al. 2012), and ice core data from the Greenland Ice Core Project (GRIP, Johnsen et al. 1992, 1997).

Long-term air temperature and precipitation data were ~~taken~~obtained from the SeaRISE project (Sea-level Response to Ice Sheet Evolution; http://websrv.cs.umt.edu/isis/index.php/SeaRISE_Assessment, Bindshadler et al. 2013), which provided a baseline for climatic changes over the last 125 thousand years from the Last Interglacial to the present day (the latter date set as 1950). This dataset was chosen because it was the only gapless time series for the targeted 125 thousand-year period

available at the time of model integration. ~~In order to~~To determine detailed changes for more recent years (i.e~~.~~, after year 850), we incorporated simulation results from the PMIP3, especially from past millennium runs for the years 850 to 1850 (Braconnot et al. 2012) and historical runs after the year 1850 (Taylor et al. 2012). ~~For data after the year 1900, we~~We used reanalysis data, the University of Delaware reconstruction product (*UDel_AirT_Precip*. Willmott and Matsuura 2001), and ERA-Interim reanalysis data (Dee et al. ~~2011).~~2011) for the period following the year 1900.

The Global Land Data Assimilation System (GLDAS, Rodell et al. 2004) was used to determine hydrologic and soil parameters. After a preliminary analysis of the hydrological outputs of the four models~~;~~ (Noah, CLM, VIC, and Mosaic models), we selected the Mosaic model outputs because ~~these showed the best settings and~~ they yielded optimum results for cold regions north of 50°N with respect to evaporation and runoff response to different soil types in the examined range of temperature, -30 ℃ to 15 ℃ (Rodell and Beaudoing 2007, https://disc.gsfc.nasa.gov/datasets/GLDAS_MOS10SUBP_3H_001/summary, accessed January 23, 2020). The soil type at each grid point was determined from the 'basic soils information' ~~given~~ in the GLDAS dataset. The original 13 categories of soil type classes (other than 'water', 'bedrock', and 'other') were aggregated in the model into three major classes, i.e~~.~~, sand, silt, and clay.

Two ecological data sources were used for carbon input parameterization. The first is the result of stage 2 of the GRENE-TEA model intercomparison project (GTMIP, Miyazaki et al. ~~2014~~2015), which compares the performance of several biogeochemical models regarding the ecosystem carbon budget for the period 1850–2100. The second is the observational dataset compiled from tropical to sub-Arctic Asian sites, "The compilation dataset of ecosystem functions in Asia (version 1.2)" (personal communication, TM Saitoh, Gifu University).

~~Construction of driving and boundary conditions for integration was based on these data, as described in section 2.3.~~

The model simulation results were compared with the following datasets: simulated SOC, with the total SOC amount data compiled by Olefeldt et al. (2016, hereafter O16). Similarly, simulated ICE was compared with the dataset compiled by Brown et al. (1998, hereafter IPA-ICE), which is the only currently available distribution data covering the entire circum-Arctic area. Note that the IPA-ICE data categorises ICE distribution according to volumetric content, i.e. none, 0%–10%, 10%–20%, or over 20%, depending on the type of overburden.

2.2 Model description

The model SOC-ICE-~~0~~1v1.0 consists of two boxes: the 'above-ground' box and the 'subsurface' box (Fig. 1). The above-ground box is driven by mean annual air temperature (MAAT) and annual total precipitation (Precip~~),~~) and has attributes such as latitude, longitude, altitude, distance from the closest ocean body, presence or absence of ice sheet cover, and background carbon dioxide concentration. The model diagnoses seasonality and frozen ground state and calculates the

amount of carbon supply to the subsurface box. The subsurface box updates SOC, soil moisture, and ICE quantities, according to inputs passed from and climatic conditions determined by the above-surface box. The model was coded in Interactive Data Language（IDL, Harris Geospatial Solutions, Inc.). Sample model codes and associated data are provided as supplementary materials.

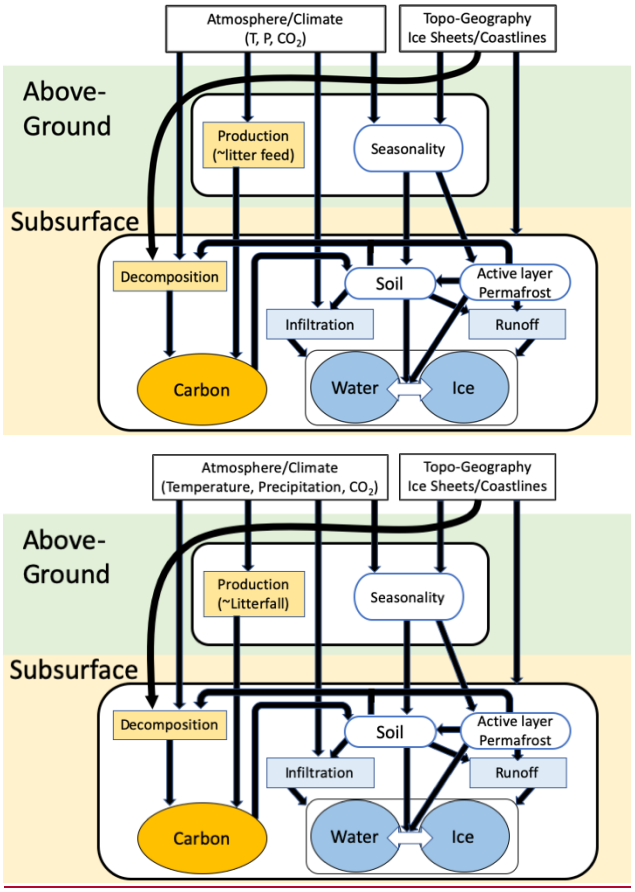

Figure 1: Schematic ~~diagram~~ of the ~~conceptual~~ numeric model SOC-ICE-~~01~~v1.0 to calculate soil organic carbon (SOC) and ground ice (ICE) budget.

2.2.1 Above-ground processes

The above-ground box calculates 1) seasonality from local ~~annual mean temperature~~MAAT and its location information (continentality), and 2) the amount of carbon supply, as litter fall, to the subsurface box.

Seasonality and presence of frozen ground

~~Since~~As the reconstructed temperature data from the SeaRISE project, T_a, are obtained on an annual basis, they do not resolve the issue of seasonality, which is important in inferring the subsurface thermal state (i.e~~,~~, presence of permafrost, seasonal freezing, or no freezing of ground) (Saito et al. 2014, 2016, Harris 1981). We derived simple relationships between T_a and seasonal amplitude T_{amp} as a set of functions of location (longitude, latitude), ~~closest ocean,~~ distance from the coast of the closest ocean, and background climatic state, i.e~~,~~, glacial (cold) or interglacial (warm) (Supplementary Fig. 1). For the warm period (defined in this study as 125 ~~ka~~ to 100 ka~~,~~ and ~~14 ka~~after Bølling-Allerød interstadial to the present day, judged by changes in reconstructed temperature and sea level data), the present-day climate was assumed to provide typical variations, and monthly data ~~taken~~obtained from the ERA-Interim reanalysis were used. In contrast, monthly data ~~taken~~obtained from the six PMIP3 models for the LGM simulations were used to derive average climatology for the cold periods (100 ka to 14 ka). The six models were selected ~~so that they~~to provide simulation results for both the LGM and the Holocene Climate Optimum (mid-Holocene run, 6 ka): CCSM4 (Gent et al., 2011), CNRM-CM5 (Voldoire et al. 2011), IPSL-CM5A-LR (Dufresne et al. 2013), MIROC-ESM (Watanabe et al., 2011), MPI-ESM-P (Brovkin et al., 2013), and MRI-CGCM3 (Yukimoto et al., 2012). ~~Since~~Because of the horizontal resolution and the sea/land mask differed between models, coastlines were determined for each model from ~~altitude data.~~its orography condition. Assuming the sinusoidal seasonal changes in temperature $T_a + T_{amp} \sin t$, the freezing and thawing indices (FDD and TDD, respectively) were calculated as the cumulative degree day of the temperature below and above 0 °C. The type of underlying frozen ground was then identified based on the classification method developed by Saito et al. (2014, 2016) as climate-driven permafrost (CP, corresponding to continuous permafrost), environmentally-conditional permafrost (EP, corresponding to discontinuous permafrost), long-lasting seasonally frozen ground (Sf), intermittently frozen ground (If, frozen for a short duration, i.e~~,~~, less than two weeks), or not frozen (Nf).

Litter fall

The amount of carbon supply to the subsurface box, calculated as litter fall (in kgC m^{-2} a^{-1}), was determined by the combination of MAAT T_a and Precip P_r (Figure 3a.). For simplicity, we did not incorporate carbon type differences inherent in plant functional types (De Deyn et al. 2008). The shape of the litter fall function was determined by fitting the outputs of the biogeochemical models ~~taken~~obtained from the GTMIP stage 2 project (Fig. 2a–d), i.e~~,~~, VISIT (Ito 2019), B-BGC (Thornton et al. 2002), SEIB-N (Sato et al. 2016), and CHANGE (Park et al. 2011). Relatively small values of SEIB-N, likely because of its biomass growth still being underway for this integration (cf. Figure S3 in Pugh et al. 2020), did not change the resulting shape significantly. The derived function was then adjusted by multiplying it by a constant value to the best-fit (in terms of least square errors), to the observational data 'The compilation dataset of ecosystem functions in Asia (version 1.2)' ~~(personal communication, TM Saitoh, Gifu University).~~ The resulting equation was formulated as follows:

$$LitterFall(T_a, P_r, CO_2) = a_1(co_2)\ exp\left(-\frac{(T_a - T_0)^{c_T}}{b_T}\right) \cdot log\left(\frac{P_r + P_0}{b_P}\right), \quad (1)$$

where $T_a(t)$ and $P_r(t)$ denote the values of MAAT and Precip, respectively, of the location in a year, t. T_0 and P_0 are the respective baseline values. a_1, b_T, c_T, and b_P are shape parameters. These parameters were determined by curve-fitting to the model outputs (Fig. 2a–d) and observations; a_1 and b_T vary depending on the background atmospheric concentration of carbon dioxide CO_2 [ppm]. The values of these parameters and baseline values used in this study are summarised in Table 1. An example of the litter fall distribution under present-day climate conditions is shown in Fig. 2e.

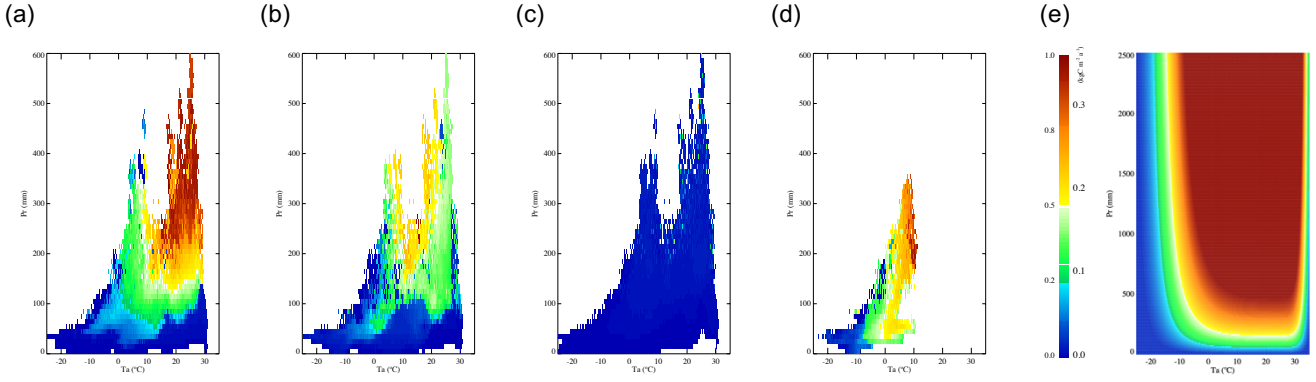

Figure 2. Distribution of litter fall, ~~the~~ carbon input to the "sub-surface" box, for a given mean annual air temperature (Ta) and annual total precipitation (Pr) pairs. a) Distribution of litter fall outputs calculated by biogeochemical models and normalized to the respective maximum value: a) VISIT, b) Biome-BGC, c) SEIB-N, and d) CHANGE for global land areas, except for CHANGE, the result of which covered only land areas north of 50°N. The scale is shown on the left-hand side of the colour bar. e) Modelled litter fall distribution based on simulated outputs for the functional shape and calibrated for absolute value by observation data. Note the vertical ranges are different for e). The scale is shown on the right-hand side of the colour bar.

2.2.2 Subsurface processes

The subsurface box has four major functions, 1) SOC budget, 2) water budget in the liquid phase, 3) assessment of freezing and thawing depths, and 4) phase change between ice and water. The box is not resolved for depth with explicit layering but an active area is assumed to be 3 m deep for hydrological calculations.

SOC budget

Accumulation and decay of organic carbon in the subsurface box ~~is~~are expressed as a difference equation, adopting Clymo's (1984) peat accumulation model for the catotelm. The change in SOC~~, SOC_n~~ in the n^{th} year, SOC_n, is formulated as Eq. (2).

$$\frac{\Delta SOC_n}{\Delta t} = LitterFall(T_a, P, CO_2) - \kappa_n \cdot SOC_{n-1}, \quad (2)$$

where $LitterFall$ [kgC m^{-2} a^{-1}] is the amount of organic carbon deposited on the ground as calculated using Eq. (1), and κ is the decomposition rate of SOC [a^{-1}], determined at each step by the following relaxation method:

$$\kappa_n = \kappa_{n-1} + \frac{(\kappa_{crit,\,n} - \kappa_{n-1})}{\tau} \cdot \Delta t. \quad (3)$$

The critical equilibrium rate of decomposition, $\kappa_{crit,\,n}$, defined as $SOC_n / LitterFall_n$, demonstrates that carbon supply from the above-ground box and the output (subsurface decomposition) of organic carbon are in balance under the given climate condition. Eq. (3) suggests that the instant decomposition rate approaches the critical equilibrium value on the time scale defined by τ. ~~In this study,~~This is the key parameter for the examination of climate and topo-geographic controls on soil carbon evolution, and we set the values of τ in this study in a geometric series at 4, 20, 100, and 500 yr, adhering to ~~examine climate and topo-geographic controls on soil carbon evolution, after following~~ considerations. Although closely related, τ does not represent the soil turnover (e.g.~~,~~, from tens to thousands of years; Perruchoud et al. 1999, Conant et al. 2011, Luo et al. 2019) or ecological secondary succession (e.g.~~,~~, from ~~some~~a few years to tens of years ~~after~~following wildfire in permafrost areas; Yohikawa et al. 2003 and Narita et al. 2015~~,~~; or from tens to hundreds of years under temperate conditions; Svenning and Sandel 2013). It is a hypothetical variable representing the time scale for decomposition to approach ~~to~~ its equilibrium value under the given climate and topo-geographic condition. For peatlands in the taiga and tundra that lie between subarctic and arctic regions, it may take ~~longer~~more than a thousand years to reach an equilibrium ~~due~~, owing to the slow plant growth and carbon decomposition because of the cool and/or dry environment, ~~while~~whereas it can happen in ~~a~~ yearly order, $O(1\ year)$, in warm and moist tropical rainforests, where the fast cycle of vegetation growth/death and decomposition facilitates rapid changes (Harden et al. 1992; Vitt et al. 2000a). We also incorporated impacts of permafrost presence and wetness of the ground on SOC dynamics by specifying a larger value of τ, determined according to frozen and/or wet conditions (e.g.~~,~~, 2500 yr for saturated frozen ground in continuous permafrost zones and 1500 yr for saturated frozen ground in discontinuous permafrost zones).

Table 1. List of parameters used in the model

Eq.	Category			Remarks
(1)	Litter fall	a_1	$1.2\left\{1. - \left(0.808 - \frac{CO2}{1000.}\right)^3\right\}$	

		T_0	25.0	baseline Ta [°C]
		b_T	$10.^{\wedge}\left(2.14+3.10\frac{CO2}{1000.}\right)$, if $T_a > T_0$ 4.5×10^5 otherwise	
		c_T	4.0	
		b_P	5.0	
		P_0	160.0	baseline Pr [mm]
(4)	Hydrology	γ	0.61 ~ 0.99	infiltration ratio [-], depends on soil type, temperature, and frozen state
		ξ	0.09 (sand), 0.045 (silt), 0.~~09~~03 (clay)	base runoff ratio [-]
(7)	Thermal conductivity	k^{peat}	0.01	for peat [W m^{-1} K^{-1}]
		k^{mnl}	1.2	for mineral soil [W m^{-1} K^{-1}]
		k^{water}	0.6	for water [W m^{-1} K^{-1}]
		~~k^{pice}~~ k^{ic}	2.2	for ice [W m^{-1} K^{-1}]
(8)	Soil column	h_b	3000.	soil column depth [mm]
		σ	0.55 (sand), 0.50 (silt), 0.45 (clay)	porosity [-]

Hydrological process

Figure 3 shows a schematic ~~diagram~~ of the subsurface hydrological model for exposed land (i.e~~.~~, not covered by ice sheet or water). The budget of the liquid-phase water W_n is controlled ~~by~~using Eq. (4) as the balance between the input (the first term on the righthand side) and the output (the second and third terms).

$$\frac{\Delta W_n}{\Delta t} = \gamma P - \xi W_{n-1} - \varphi_n. \quad (4)$$

The first term in Eq. (4) refers to annual net precipitation (i.e~~.~~, precipitation – evapotranspiration – surface runoff) with γ denoting the ratio of subsurface infiltration to the total precipitation. The second term refers to base runoff as a function of water storage in the liquid phase, and ξ is a parameter for the ratio of base runoff. The third term refers to new ice freezing or melting at a time step. Soil moisture [mm] in the active area overflows as runoff when it exceeds the saturation soil moisture ($h_a = \sigma h_b$), where σ is porosity, and h_b is the depth of the hydrologically active area set to 3000 mm in this study (Fig. 3). In contrast, the overall storage of ICE at location, I_n, has no limitation (to mimic the development of ice wedge) and is updated using Eq. (5). The computation of φ is described in the next subsection.

$$I_n = \varphi_n + I_{n-1} \quad (5)$$

295 The parameters of soil characteristics (porosity σ, infiltration rate γ, and base runoff ratio ξ of the area) are summarized in Table 1.

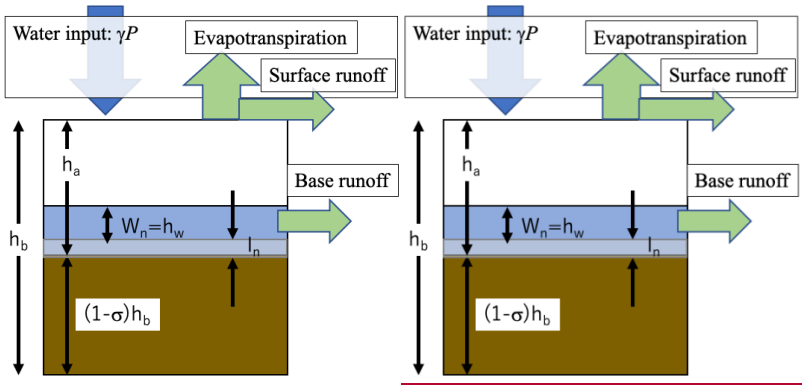

~~Figure 3. Schematic diagram for hydrological processes of the subsurface box.~~Figure 3. Schematic of hydrological processes of the subsurface box. It is a bucket-type reservoir of capacity h_b (m), consisting of liquid water ($W_n = h_w$) within the pore space ($h_a = \sigma h_b$) and soil ($(1-\sigma)h_b$). Quantity of ice forming or melting at a time step is limited by current liquid or solid water amount, respectively (Eq. 9); total amount of ice (I_n) can supersede the capacity h_b to represent massive ground ice.

Assessment of freezing and thawing depths

300 The changes in the amount of ICE, φ_n, are analysed ~~through~~by identifying the energy balance between ground freezing and thawing processes. They are set proportional to the depth of freezing d_n^f and thawing d_n^t, which are empirically determined by Eq. (6a–b) from ground thermal conductivity (for the frozen state, k_n^f, and thawed state, k_n^t, respectively) and respective freezing and thawing indices calculated in the above-ground box (i.e~~,~~. FDD and TDD).

$$d_n^f = \sqrt{\frac{2k_n^t \cdot FDD}{W_n/h_b \rho_w \cdot \lambda}} = \alpha_f \sqrt{FDD}, \tag{6a}$$

305 $$d_n^t = \sqrt{\frac{2k_n^f \cdot TDD}{W_n/h_b \rho_w \cdot \lambda}} = \alpha_t \sqrt{TDD}, \tag{6b}$$

where ρ_w is the density of water, and λ is the latent heat of fusion. Thermal conductivity is evaluated from carbon and water content using Eq. (7).

$$k_n^{t,dry} = \frac{SOC_n}{\chi^{t,dry}} k^{peat} + \left(1 - \frac{SOC_n}{\chi^{t,dry}}\right) k^{mnl}$$

$$k_n^t = \frac{W_n}{\chi^{t,wet}} k^{water} + \left(1 - \frac{W_n}{\chi^{t,wet}}\right) k_n^{t,dry} \tag{7}$$

$$k_n^f = \frac{I_n}{\chi^f} k^{ice} + \left(1 - \frac{I_n}{\chi^f}\right) k_n^t$$

where k^{peat}, k^{mnl}, k^{water}, k^{ice} denote thermal conductivity values for carbon-containing and mineral parts of the soil, water, and ice, respectively. The relative amounts of thawed dry or wet soil~~,~~ and frozen soil are defined by Eq. (8).

$$\chi^{t,dry}(SOC_n, h_b;\ \sigma) = (1-\sigma)h_b + SOC_n$$

$$\chi^{t,wet}(W_n, SOC_n, h_b;\ \sigma) = (1-\sigma)h_b + SOC_n + W_n = \chi^{t,dry} + W_n, \tag{8}$$

$$\chi^f(I_n, SOC_n, h_b;\ \sigma) = (1-\sigma)h_b + SOC_n + I_n = \chi^{t,dry} + I_n$$

Phase change between water and ice

The change in ~~ice~~the amount of ice is calculated as follows:

$$\varphi = \begin{cases} -I_n \\ \tilde{\varphi} \\ W_n \end{cases} \quad \text{if} \quad \tilde{\varphi}: \begin{cases} \cdot < -I_n \\ -I_n \le \cdot \le W_n, \\ W_n < \cdot \end{cases} \tag{9}$$

where $\tilde{\varphi}$ is ~~defined by~~expressed as

$$\tilde{\varphi} = \beta\left(d_n^f - d_n^t\right)\frac{W_n}{h_b}. \tag{10}$$

β is a parameter ~~to control~~that controls the distribution of energy in melting or freezing of water, $\beta_{freeze} = 0.5$; $\beta_{thaw} = 1.0$. The parameter values not listed here are summarised in Table 1.

2.3 Driving and boundary condition data

The model is driven by inputs of MAAT, Precip, and atmospheric carbon dioxide concentration, along with geographical information: longitude, latitude, continentality, and land condition types (i.e~~,~~, exposed land, under water, or under ice sheets). In this study, the model was integrated for the last 125 thousand years north of 50° in the Northern Hemisphere with 1-degree resolution, aligning with the grid system of the employed dataset for ice sheet evolution (i.e~~,~~, ICE-6G_C).

2.3.1 Forcing data for 125 thousand years

The baseline 125 thousand-year time series of annual temperature and precipitation was ~~taken~~obtained from the SeaRISE (Sea-level Response to Ice Sheet Evolution; Bindshadler et al. 2013) project. The time series presents deviations from current mean temperature~~,~~ or ratios to the current precipitation amount. The SeaRISE time series ~~needs~~requires present-day

climatology data for a specific location. The present-day climatology was computed from ERA-Interim reanalysis data for the years 1979–2016. Moreover, the SeaRISE time series has low temporal resolution in the recent millennium (i.e~~.~~, 100-yr intervals). We examined the SOC time series calculated using the forcing data obtained from the CMIP5/PMIP3 models for ~~overall goodness of the reproduced time series in the circum-Arctic region~~the period (the Last Millennium and ~~used~~the historical runs), with respect to the mean values, temporal variability and smooth connectivity to the historical period, to select the IPSL simulation results. The ~~past climate anomaly time series~~SeaRISE data for the period 850–1850 was ~~refined~~replaced by the outputs from its '~~last millennium'~~Last Millennium' run~~,~~ and that for the period 1850–1900 by its 'historical' run. Similarly, the anomaly time series for the period 1900–2006 was constructed using the University of Delaware reconstruction product (*UDel_AirT_Precip*).

(a) (b) (c)

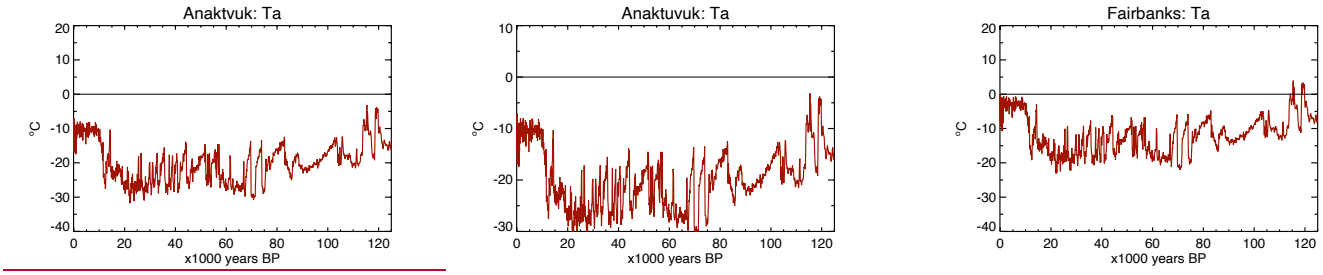

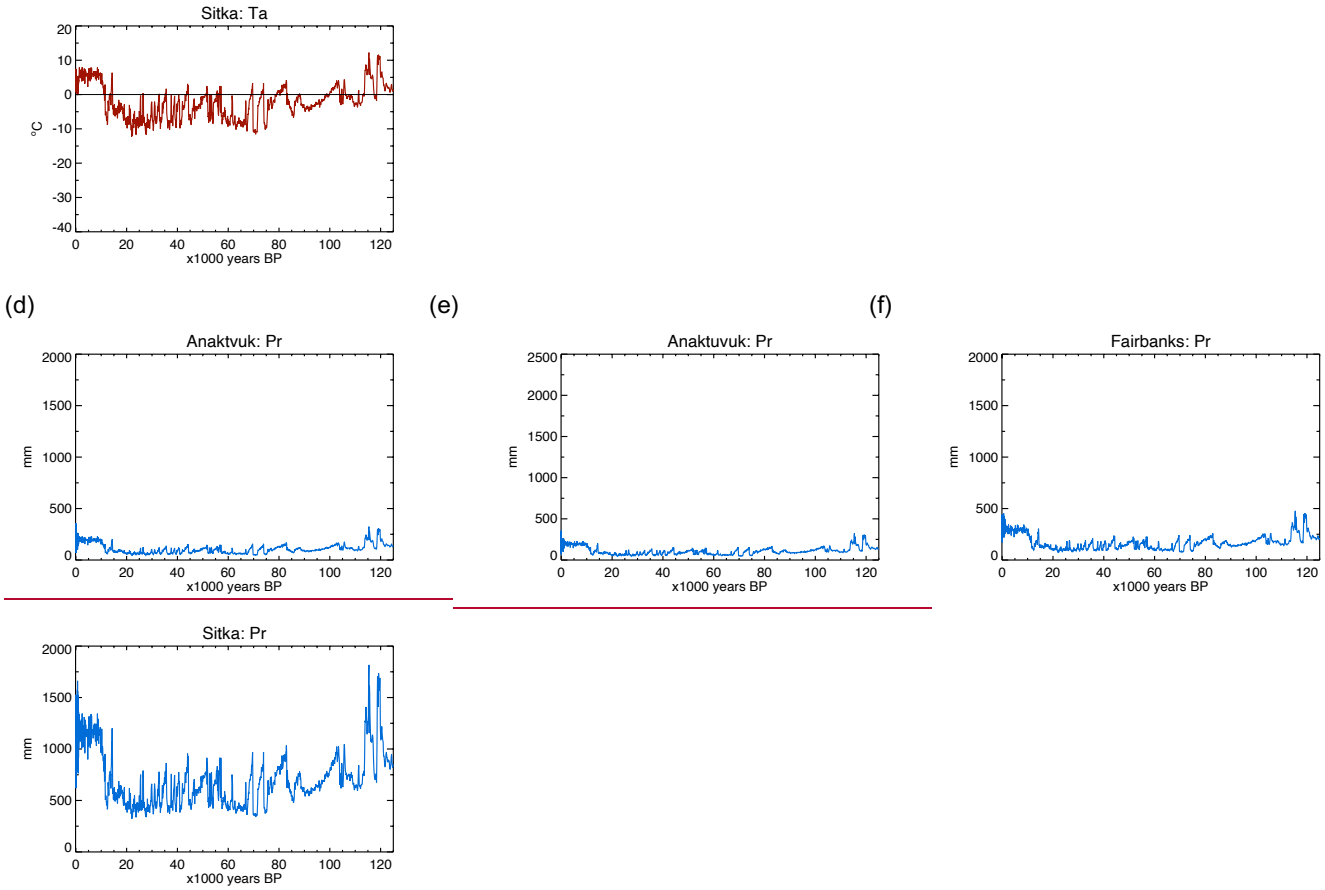

Figure 4: Example time series of climate forcing data (temperature, precipitation~~), and diagnosed litter fall.~~). The temporal variations in climate forcing data were reconstructed from Greenland ice-core data (the SeaRISE project), while present-day climatology at the 1-degree grid point was derived and interpolated from ERA-Interim reanalysis. The litter fall time series were computed from Eq. (1). Mean annual air temperature (~~MAAT~~Ta; in ºC) at the Alaskan grid point closest to a) Anaktuvuk (69.5ºN), b) Fairbanks (64.5ºN), and c) Sitka (57.5ºN). d), e), and f) Same as a), b), and c) except for annual total precipitation (Pr; in mm).

Considering the meridional dependence (i.e~~.~~, polar amplification effect) of δT_a, the amplitude of temperature variations between glacial and interglacial periods and the amplitude of the SeaRISE anomaly temperature time series were reduced southward within the 50 and 70 meridional band at a rate of 0.25 °C per 1 degree from its original value, 23.3 °C, which was determined by preliminary analysis on $[\partial(\delta T_a)/\partial\, lat]$ for six PMIP3 models (Supplementary Fig. 2). These time series were then combined with present-day climatology to produce a 125 thousand-year time series for each 1-degree resolution grid point. Examples of the reconstructed time series of temperature and precipitation for three different locations in Alaska are shown in Fig. 4.

2.3.2 Boundary conditions

For the last 125 thousand years of the integration period, there have been substantial changes in the presence and thickness of ice sheets, as well as in altitudes and coastlines, in the circum-Arctic area. These surface boundary conditions ~~exert a large influence on~~significantly affect the calculation of subsurface carbon and ice dynamics through various processes such as submergence, uplift, burial under ice sheets, and removal by glacial dynamics. We used the ICE-6G_C datasets (Argus et al. 2014, Peltier et al. 2015) to determine altitude, the areal ratio of land, water, and ice cover, and ice thickness for the original 1-degree grid points. Each grid point has three sections, i.e~~,~~, exposed land, under ice, and under water (e.g~~,~~, sea, lake), following the areal fraction of land and ice of the dataset. The amounts of carbon, ice, and water are reshuffled due to changes in land cover fractions, in addition to the internal dynamics of carbon and water determined by Eqs. 2 and 4. ~~When some portion of the grid becomes ice-free (melting of ice sheet), water from the melting ice is added to the precipitation input (in Eq. 4), and the SOC amount corresponding to the newly exposed areal fraction is lost from the grid's storage to reflect basal ablation.~~ When some portion of the grid submerges, the SOC amount and ice content, as well as frozen ground condition, belonging to this areal portion ~~are kept~~remain unchanged but the water content to the portion becomes saturated. Similarly, SOC and ICE remain unchanged under ice sheets except when some portion of the grid becomes ice-free (melting of ice sheet). In such cases, water from the melting ice is added to the precipitation input (in Eq. 4) and the SOC amount corresponding to the newly exposed areal fraction is lost from the grid's storage to reflect basal ablation.

2.3 ~~Results~~

~~The amounts of SOC, ICE,~~3 Initial values and ~~soil moisture were computed using~~spin-up

We examined the ~~SOC ICE 01~~ model's sensitivity to initial values with a small set of different SOC (namely, 5.0, 10.0, 20.0, 22.5, 25.0, 27.5, 30.0, 50.0, and 100.0 kgC m^{-2}) and soil moisture (100, 500, 1000, 1500 mm for the 3000 mm column) values in limited locations (cf. Fig 5a). The model sensitivity showed clear dependency~~. The calculation was performed~~ on the ~~1 degree interval grid system.~~ initial values of SOC but was negligible for soil moisture. Based on this preliminary examination, we determined the initial values that would produce the most realistic range for the present-day circum-Arctic, namely 25.0 kgC m^{-2} for SOC and 500 mm for soil moisture.

Before full integration, the model was spun up ~~by~~(or equilibrated) for a certain period of years to attain an internal balance in the SOC, soil moisture and ICE budget with the forcing. We integrated the model for 5000 years for spin-up with the constant ~~initial~~ forcing and ~~using~~perpetual boundary data ~~for 5000 yr,~~taken from the 125 ka condition, starting from the uniform initial values of 25.0 kgC m^{-2} of SOC and 500 mm of soil moisture at all grid points to reach an equilibrated state.

2.3.4 Locations for model examinations

The behaviour of the model was evaluated in terms of the simulated 125-kyr time series for selected locations and the regional characteristics for different circum-Arctic regions.

The simulated time series of the SOC, ICE, and soil moisture were examined at the selected eight locations with different climatic characteristics for the 125-kyr period. The locations denote the grid points closest to each specified site shown in Fig. 5a. Of these, three sites are in Alaska: Anaktuvuk on the North Slope (continuous permafrost, Jones et al. 2009, Hu et al. 2015, Iwahana et al. 2016), Fairbanks in Interior Alaska (discontinuous permafrost, Miyazaki et al. 2015, Sueyoshi et al. 2016), and Sitka in southeast Alaska on the Pacific coast (seasonally frozen ground). Sitka is the warmest and most pluvial site of the eight. Two sites are in Canada: Yellowknife by the Great Slave Lake in the Northwest Territories (discontinuous permafrost) and Churchill in Hudson Bay Lowlands (continuous permafrost, Dyke and Sladen 2010, Sannel et al. 2011). Both of these were under the Laurentide Ice Sheet during the Last Glacial period and started carbon accumulation after deglaciation at different times (Dyke 2005). Three sites are in Eurasia. Kevo in northern Finland (Miyazaki et al. 2015, Sueyoshi et al. 2016), which was covered by the Fennoscandia Ice Sheet during the Last Glacial period, has oceanic influence and locates in the discontinuous permafrost zone. Omsk in southwestern Siberia (seasonally frozen ground) has continental characteristics and has been ice-free. Yakutsk is in East Siberia (continuous permafrost, Miyazaki et al. 2015, Sueyoshi et al. 2016). Anaktuvuk and Yakutsk are obtained from areas where the ice-rich permafrost can be found (Murton et al. 2015, Kanevsky et al. 2011). Geographical and climatological data of these locations are shown in the two leftmost columns in Table 2.

Further, we specified eight circum-Arctic regions to compare the simulated carbon and ice dynamics with values reported in the literature (Yu et al. 2009, Smith et al. 2004, McDonald et al. 2006, Jones and Yu 2010). The locations and areas of these eight regions are as follows: Alaska (high latitudes) (67.5–73.5°N, 169.5–139.5°W), Alaska (middle latitudes) (62.5–67.5°N, 169.5–139.5°W), Alaska (low latitudes) (59.5–62.5°N, 169.5–139.5°W), West Canada (high latitudes) (60.5–69.5°N, 129.5–103.5°W), West Canada (low latitudes) (51.5–60.5°N, 129.5–103.5°W), East Canada (44.5–62.5°N, 73.5–59.5°W), Finland (60.5–68.5°N, 22.5–27.5°E), and West Siberia (55.5–60.5°N, 72.5–84.5°E) (Fig. 5b).

(a) (b)

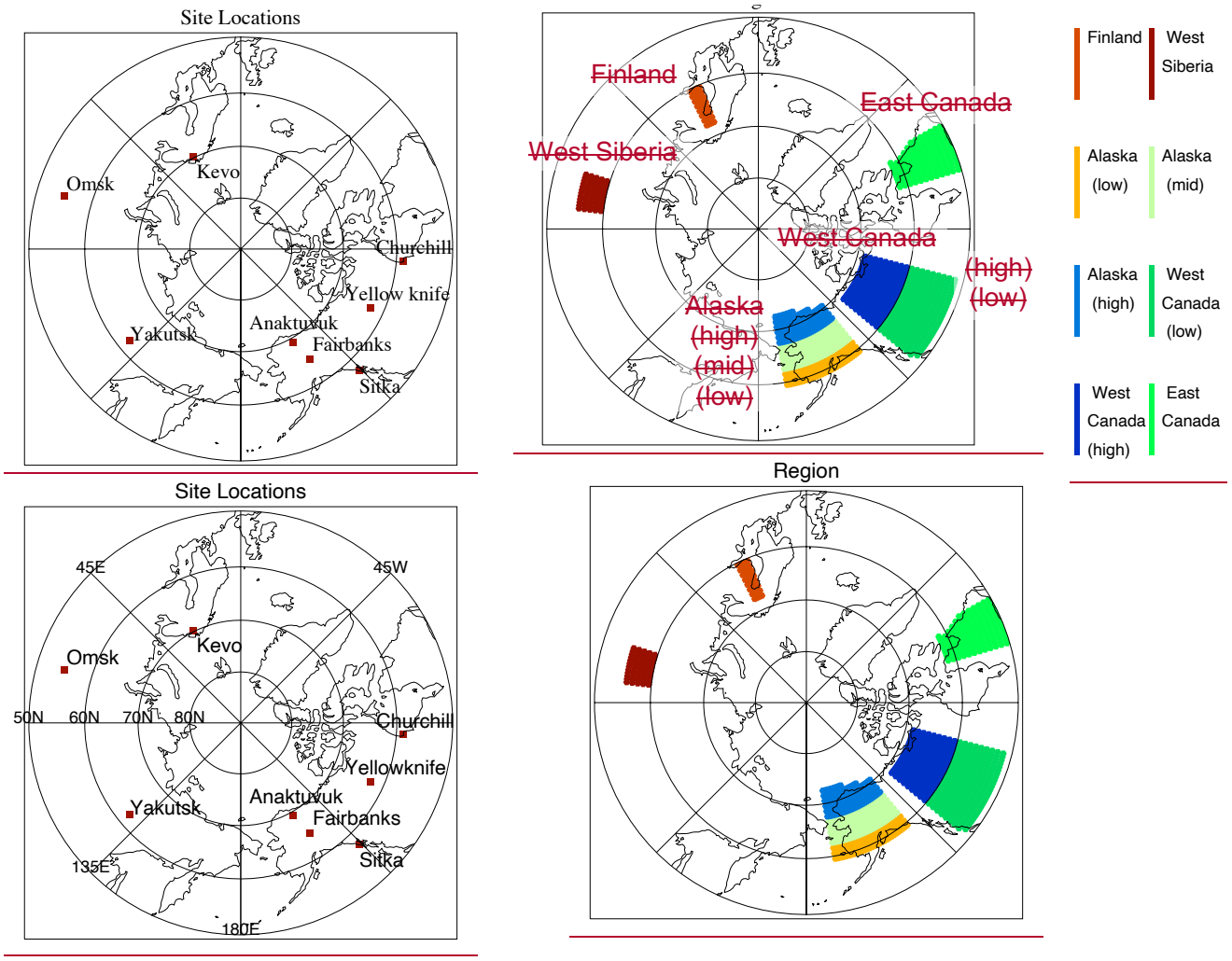

Figure 5: a) Locations of the eight ~~examples~~sample sites for comparison of simulated time series. b) Areal extents of the eight sub regions for analysis of the accumulation history of SOC and ICE.

420

425

Table 2. Comparison of simulated SOC and ICE with observation-based data for eight locations ~~(longitude and~~ . Longitude, latitude ~~denote~~, the climatology of mean annual air temperature (Ta) and annual total precipitation (Pr), and the simulated results are obtained from the values of the nearest 1 ~~degree~~ ^{o} resolution grid point~~).~~. τ denotes the relaxation time scale of decomposition rate.

Locations	Soil[a)]	Var.	Obs-based[b)]	$\tau = 4$	$\tau = 20$	$\tau = 100$	$\tau = 500$
Anaktuvuk (69.5°N, 150.5°W) Ta: -8.510.1 °C, Pr: 175150 mm	silt	SOC[c)]	66.3	48.7	48.7	48.7	44.6
		ICE[d)]	10-20%	30.6	30.6	30.6	30.6
		SM[e)]	0.56	0.92	0.92	0.92	0.92
Fairbanks (64.5°N, 147.5°E) Ta: -3.12.2 °C, Pr: 246273 mm	silt	SOC	43.8	13.7	17.7	25.0	39.8
		ICE	0-10%	0.3	0.3	0.3	0.3
		SM	0.54	0.78	0.78	0.78	0.78
Sitka (57.5°N, 135.5°W) Ta: 5.36.2 °C, Pr: 6571156 mm	silt	SOC	0.0	1.0	3.1	13.1	30.3
		ICE	0%	0.0	0.0	0.0	0.0
		SM	0.28	0.52	0.52	0.52	0.52
Yellowknife (62.5°N, 114.5°W) Ta: -6.94.5 °C, Pr: 96147 mm	silt	SOC	14.1	11.7	15.0	23.7	35.6
		ICE	10-20%	20.3	20.3	20.3	20.2
		SM	0.84	0.87	0.87	0.87	0.87
Churchill (58.5°N, 94.5°W) Ta: -8.86.1 °C, Pr: 224234 mm	silt	SOC	166.8	23.7	26.6	33.7	36.5
		ICE	10-20%	28.5	28.5	28.5	28.5
		SM	0.73	0.49	0.49	0.49	0.49
Kevo (69.5°N, 27.5°E) Ta: -0.62 °C, Pr: 181285 mm	sand	SOC	60.1	0.4	4.4	17.6	38.4
		ICE	0-10%	0.0	0.0	0.0	0.0
		SM	0.43	0.07	0.07	0.07	0.07
Omsk (54.4°N, 73.5°E) Ta: 0.42.2 °C, Pr: 207202 mm	clay	SOC	-[f)]	6.5	9.4	13.2	34.4
		ICE	0%	0.0	0.0	0.0	0.0
		SM	0.9	0.74	0.74	0.74	0.74
Yakutsk (62.5°N, 129.5°E) Ta: -11.59.3 °C, Pr: 138131 mm	silt	SOC	70.2	39.0	39.0	39.0	40.9
		ICE	10-20%	16.2	16.2	16.2	16.2
		SM	0.24	0.59	0.59	0.59	0.59

Climatology of temperature (Ta) and precipitation (Pr) is the average of the driving data for the period 1981–2010.

a) Soil types are determined from the basic soils information used for the 1-degree resolution Global Land Data Assimilation System (GLDAS. Rodell et al. 2004) dataset (https://ldas.gsfc.nasa.gov/gldas/soils. Accessed on March 10, 2020).

b) Soil organic carbon amount is ~~taken~~obtained from Olefeldt et al. (2016); Ground ice content category is ~~taken~~obtained from Brown et al. (1998). In both cases, the values of the nearest grid point were used.

c) Observation-based and simulated ~~Soil~~soil organic carbon is in kgC m^{-2}.

~~d) Simulated ground ice is in meter.~~

d) Ground ice is shown in categorical volumetric percentage for the observation-based quantity, while simulated values are shown in terms of ice thickness in metre.

e) Soil moisture in terms of saturation ratio was calculated respectively from the GLDAS Mosaic product (assimilated data) and the SOC-ICE~~-01~~-v1.0 results, assuming the same porosity.

f) No data was found in the vicinity.

~~**Here, we examined the behaviour of the simulated time series for SOC, ICE, and soil moisture through the glacial and interglacial periods at the selected eight locations with different climatic characteristics in the circum-Arctic regions**~~**3 Results and discussions**

The amounts of SOC, ICE, and soil moisture were computed using the SOC-ICE-v1.0 model. The calculation was performed on the 1-degree interval grid system. Here, we have examined the simulated time series for SOC, ICE, and soil moisture through the glacial and interglacial periods in the circum-Arctic regions and have discussed the behaviour of the model.

~~. The locations denote the grid points closest to each specified site shown in Fig. 5a. Of these, three sites are in Alaska: Anaktuvuk on the North Slope (continuous permafrost, Jones et al. 2009, Hu et al. 2015, Iwahana et al. 2016), Fairbanks in Interior Alaska (discontinuous permafrost, Miyazaki et al. 2013, Sueyoshi et al. 2014), and Sitka in southeast Alaska on the Pacific coast (seasonally frozen ground). Sitka is the warmest and most pluvial site of the eight. Two sites are in Canada: Yellowknife by the Great Slave Lake in the Northwest Territories (discontinuous permafrost) and Churchill in Hudson Bay Lowlands (continuous permafrost, Dyke and Sladen 2010, Sannel et al. 2011). Both of these were under the Laurentide Ice Sheet during the Last Glacial period and started carbon accumulation after deglaciation at different times (Dyke 2005). Three sites are in Eurasia. Kevo in northern Finland (Miyazaki et al. 2013, Sueyoshi et al. 2014), which was covered by the Fennoscandia Ice Sheet during the Last Glacial period, has oceanic influence and in the discontinuous permafrost zone. Omsk in southwestern Siberia (seasonally frozen ground) has continental characteristics and has been ice-free. Yakutsk is in East Siberia (continuous permafrost, Miyazaki et al. 2013, Sueyoshi et al. 2014). Anaktuvuk and Yakutsk are in areas that include the ice rich permafrost (*Yedoma*) region (Murton et al. 2015, Kanevsky et al. 2011). Geographical and climate data of these locations are shown in Table 2.~~

3.1 Time series analysis

Table 2 shows the results of the simulated present-day contents and corresponding observation-based data at the eight selected locations with respect to SOC, ICE, and soil moisture (relative to the saturation level). In Table 2, the calculated SOC contents with different values of τ are compared with O16 total SOC amount ~~compiled by Olefeldt et al. (2016)~~ at the nearest point. The computed ICE content was compared with ~~ground ice information compiled by Brown et al. (1997), which is the only currently available distribution data covering the entire circum-Arctic area. Note that Brown et al. (1997) categorised~~ IPA-ICE ~~distribution by volumetric content, i.e., none, 0–10%, 10–20%, or over 20%, depending on the type of overburden~~. The larger the value of τ, the larger the simulated SOC amount for the present day. On the contrary, ICE content showed almost no sensitivity to τ under current formulae (Eqs. 4–10). The resulting ranges at eight locations and inter-site variations in the simulated present-day SOC and ICE contents were largely consistent with observation-based data, except for underestimation of SOC and overestimation of ICE at the Churchill site. Moreover, the value of τ has a discernible control over the simulated present-day SOC amount for all locations except Anaktuvuk and Yakutsk, which have ~~been~~ almost entirely been in continuous permafrost zones throughout the integration period (Fig. 6).

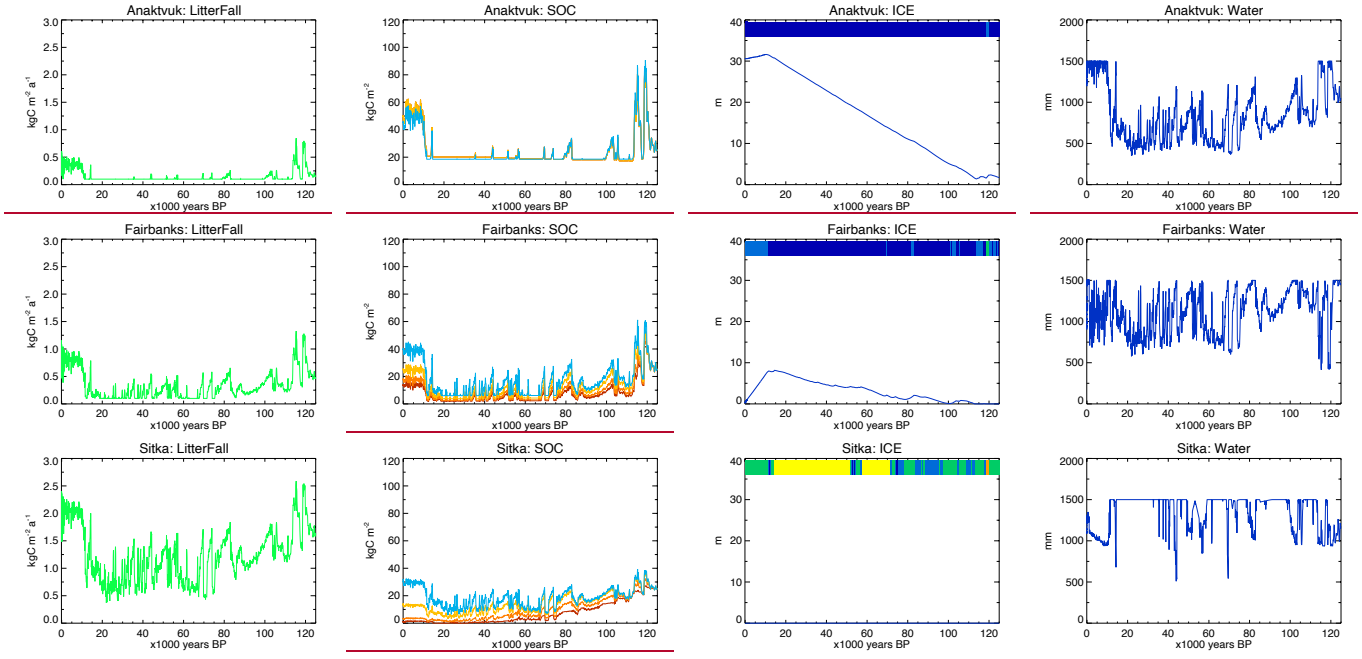

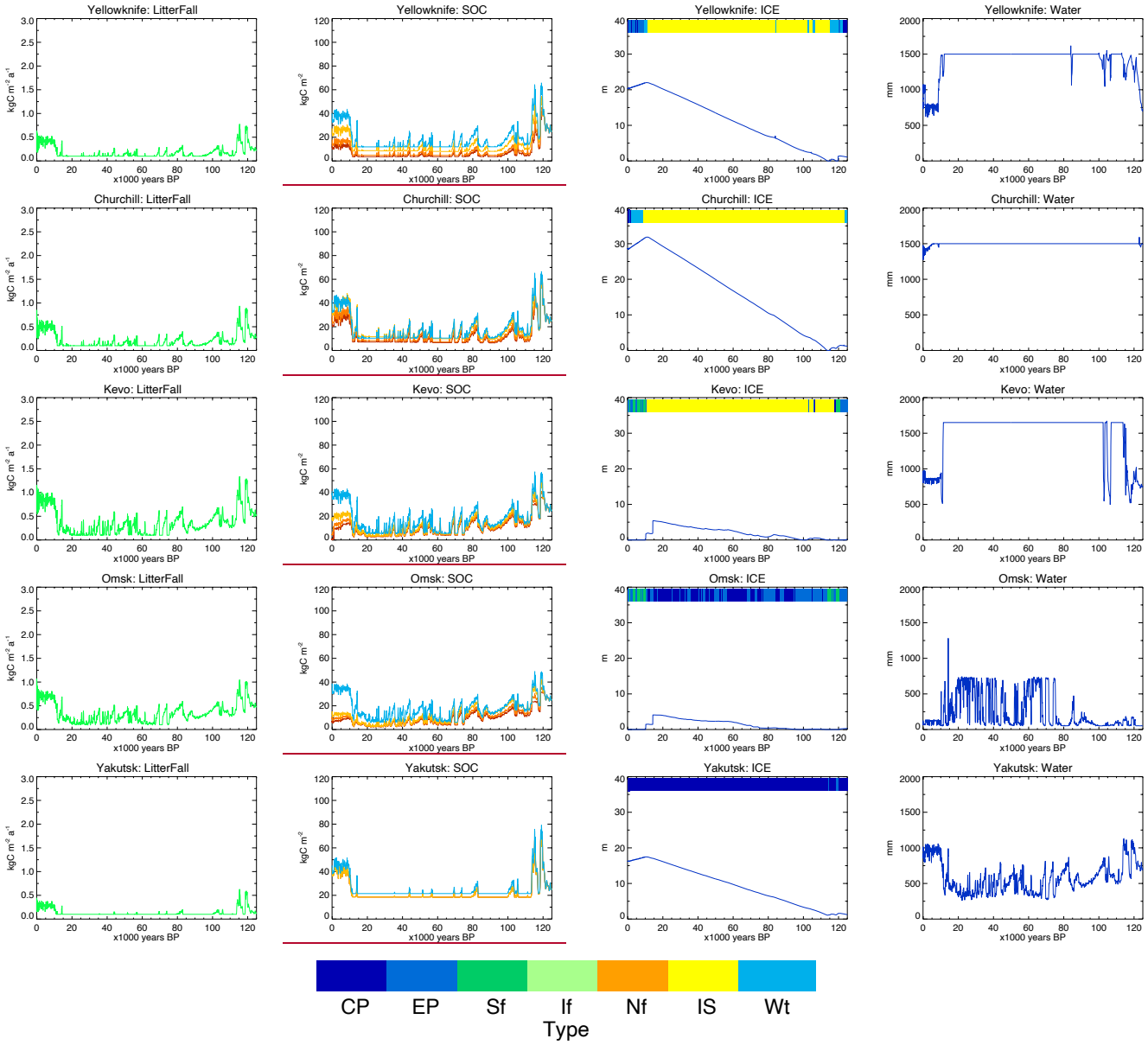

Figure 6: Results of model simulations for the eight circum-Arctic sites shown in Figure 5. 125-thousand-year time series of litter fall (in kgC m^{-2}; leftmost column), soil organic carbon (SOC in kgC m^{-2}; second from left), ground ice (ICE in ~~meters~~metre; second from right) and ~~ground water~~groundwater in liquid phase (Water in mm; rightmost column) are shown for different values of τ, relaxation time scale of decomposition rate (red: 4 years, orange: 20 years, yellow: 100 years, blue; 500 years). The legend shows land cover types for continuous permafrost (CP, deep blue), discontinuous permafrost (EP, blue), seasonally freezing ground (Sf, green), intermittently frozen ground (If, pale green), no freezing (Nf, orange), ice sheets (IS, yellow), and water body (Wt, pale blue).

3.1.1 Soil organic carbon

Figure 6 shows the 125-thousand-year ~~timeseries~~time series of model outputs for litter fall, SOC, ICE, and soil moisture at eight locations. Litter fall (the leftmost column in Fig. 6) increased ~~in proportion~~proportionally to annual temperature and precipitation (Eq. 1, Figs 2a and 4). Although the values of litter fall appeared to be larger than observed values, the resulting SOC amount and its circum-Arctic distribution did not show overestimation (see the SOC column of Fig. 6; cf. Saito et al. 2020 ~~in review~~). This result is discussed in section ~~4~~3.3.2, along with suggestions for future improvements. The simulated SOC changes showed a tendency ~~at all locations~~ for accumulation to be active during warm (i.e~~.~~, interglacial) periods and inactive during cold (i.e~~.~~, glacial) periods~~,~~ at all locations. This is consistent with existing knowledge (Vitt et al. 2000a, 2000b, Charman et al. 2015).

The carbon accumulation time series shows high sensitivity to τ, except in continuous permafrost zones, in line with the result of dependency of present-day SOC amounts on τ (Table 2). These behaviours demonstrated adequate functionality of τ to represent allogenic controls of external (i.e~~.~~, climatic, topographic and/or land composition) conditions over carbon dynamics in terms of the time required to shift to ~~an~~ equilibrium under meandering climate conditions (Loisel et al. 2017, Belyea and Baird 2006).

3.1.2 Ground ice

Accumulation of ICE ~~at some time~~ during the glacial period and its ~~decrease~~decrement after the onset of deglaciation were observed at all locations except for Sitka, where no ICE was accumulated throughout the period. In continuous permafrost zones with no ice sheet coverage, i.e~~.~~, in Anaktuvuk and Yakutsk, ICE steadily accumulated during glacial periods and persists to date, despite some melting in the ~~post-glaciation period after the LGM.~~Holocene. For sites entirely covered with land ice during the glacial period, e.g~~.~~, Yellowknife, Churchill, and Kevo, ~~accumulation of~~ ICE ~~was computed~~accumulated even under land ice. This can be interpreted as the potential amount of buried massive ice at those locations, but may ~~need~~require further consideration and/or modifications in model formulations. Moreover, ~~note that~~the absolute values of simulated ICE do not necessarily show the *in-situ* amount found in the soil layer. Rather, they indicate a relative value to be compared among different locations for contemporary spatial variations or temporal development.

3.1.3 Soil moisture

Temporal changes in soil moisture (in liquid phase) are ~~demonstrated~~presented in the rightmost column of Fig. 6. In (continuous) permafrost zones, this value should be interpreted as the amount of liquid water available in summer, not the total amount of liquid water kept unfrozen during winter or over the entire period. ~~Although it is difficult to examine~~Despite the difficulty in examining the likeliness of simulated long-term changes and inter-site differences in quantitative

comparisons with observation-based evidence due to lack of data, ~~we can still interpret~~ qualitative behaviour can be interpreted. The water level after deglaciation depended largely on precipitation amount and frozen ground type (e.g.~~,~~, continuous, discontinuous permafrost, or seasonally frozen ground). At the ~~Anaktuvuku~~Anaktuvuk and Yakutsk sites, which were underlain by cold continuous permafrost, ground was dry during the glacial period and wet in the warmer Holocene because the length of the thawing period and depth of the thawed layer were limited under glacial conditions, with most liquid water frozen and stored as ice, while the active layer was thicker and persisted longer during the Holocene. In a warmer continental location, like Omsk, the water content was higher when underlain by permafrost than when ice-free, to which the decrease in base runoff and evapotranspiration may likely contribute. In Fairbanks, which is also an interior ~~city~~location but cooler and wetter than Omsk, the average and range of temporal variations remained unchanged for the entire integration period. Greater availability of water ~~due~~owing to a wetter climate may have contributed to larger fluctuations during the Holocene than in the Omsk case. At those locations covered under land ice during the glacial time (e.g.~~,~~, Sitka, Yellowknife, Churchill, and Kevo in Fig. 6), soil moisture was saturated under ice sheets (n.b., by formulation) but commonly became drier once the ice sheets retreated.

3.2 Regional analysis for the deglaciation period

~~We examined the simulated results of carbon dynamics related characteristics, i.e., basal age distribution and accumulation rates for the post-glacial SOC accumulation. We specified eight circum-Arctic regions and compared results for these with values reported in the literature (Yu et al.~~ We also examined the regional characteristics related to the carbon and ground ice dynamics for the eight circum-Arctic regions (Fig. 5b), i.e. basal age distribution (section 3.2.1) and accumulation rates (section 3.2.2) for the post-glacial SOC accumulation, and the post-glacial ICE accumulation and dissipation (section 3.2.3).

~~2009, Smith et al. 2004, McDonald et al. 2006, Jones and Yu 2010).~~ ~~The locations and areas of these eight regions are defined as follows: Alaska (high latitudes) (67.5–73.5°N, 169.5–139.5°W), Alaska (middle latitudes) (62.5–67.5°N, 169.5–139.5°W), Alaska (low latitudes) (59.5–62.5°N, 169.5–139.5°W), West Canada (high latitudes) (60.5–69.5°N, 129.5–103.5°W), West Canada (low latitudes) (51.5–60.5°N, 129.5–103.5°W), East Canada (44.5–62.5°N, 73.5–59.5°W), Finland (60.5–68.5°N, 22.5–27.5°E), and West Siberia (55.5–60.5°N, 72.5–84.5°E) (Fig. 5b).~~

3.2.1 Basal age of carbon accumulation

Figures 7a to 7c show histograms of the basal age of post-glacial soil carbon accumulation over the entire circum-Arctic domain (north of 50°N). The ~~observational studies~~ simulated results showed ~~the~~a peak of northern high-latitude SOC initiation during the 12–10 ka period, with the unequivocal concentration of the peak (logarithmic vertical scale in Fig. 7). This is consistent with the observational studies that showed a gentler distribution of initiation after the LGM at 11–9 ka, ~~despite~~although shifted later by a millennium and with regional differences (Morris et al. 2018, Jones and Yu 2010, McDonald et al. 2006, Loisel et al. 2017, Yu et al. 2009, 2010; Smith et al. 2004). ~~In comparison, simulated results showed a similar peak of increased initiation during the same period but shifted earlier by a millennium at 12–10 ka.~~ There may be

multiple reasons for this discrepancy. One possibility is related to the forcing data. Local climatic history varied ~~from location~~according to the location (Morris et al. 2018), while climate data reconstructed from a Greenland ice core was in phase at all locations (Fig. ~~4a–c). This is also revealed by the unequivocal concentration of the initiation peak in the simulated results (n.b., the logarithmic vertical scale in Fig. 7).~~4a–c) except for the differences in timings of ice-sheet retreat or submergence. Another possibility is insufficiency in the parameterisation of carbon input (Eq. 1) and output (Eqs. 2–3). The discrepancy may also be attributed to differences or technical limitations in the determination of SOC initiation. For numerical data, the basal age can be defined precisely as the first timestep with non-zero accumulation of SOC after the LGM. The limit of detection in the laboratory may simply not work at the same ~~resolution.~~detection level. Despite these limitations, the results capture the impacts of external climatic changes (i.e~~.~~,. an allogenic control) on carbon dynamics during the deglaciation period.

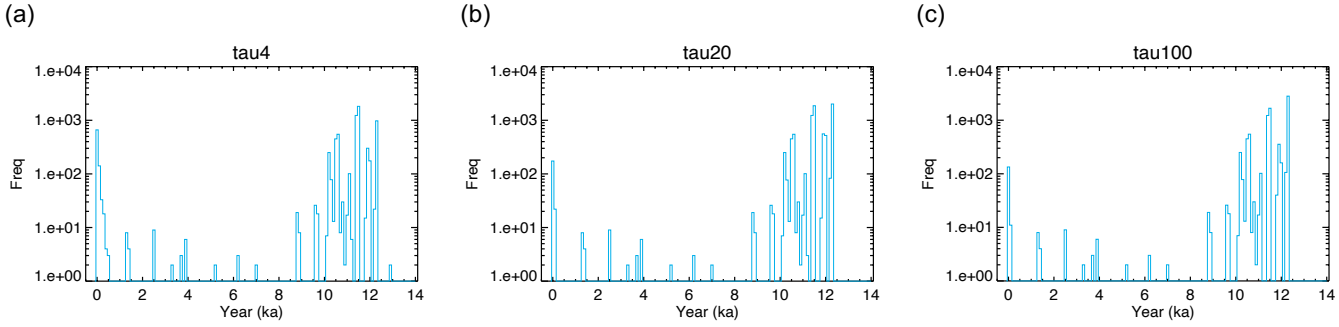

Figure 7: Histograms of circum-Arctic basal age distribution of the SOC accumulation for different values of τ: a) 4 years, b) 20 years, and c) 100 years. Ordinate (frequencies) is in the logarithmic scale.

3.2.2 SOC accumulation rates

Figure 8 shows temporal changes in the post-glacial SOC accumulation rate for eight regions (Fig. 5b). Accumulation rates were calculated from the original simulated annual time series, aggregated for regions for every millennial interval~~, and then sorted to derive percentiles. The lowest and highest whiskers of the box-whisker plots show the 10th and 90th percentiles, respectively, the lower and upper edges of the box show the 25th and 75th percentiles, respectively, and the coloured bar in the box shows the 50th percentile (median).~~. The general tendencies were reasonably reproduced such that the accumulation rate is high at 9–12 ka and in the last millennium, while it is low to modest in between (cf. Plates 3b and 5d in Yu et al. ~~2008~~2009, Figs. 1c and 3 in Yu 2012). ~~The average accumulation rate is estimated as 18.6 gC m^{-2} a^{-1} for the Northern Hemisphere extratropical climate in the Holocene (~~Yu et al. ~~2009). Simulated~~(2009) reported the observation-based estimates of topical and local accumulation rates ~~for~~in different circum-Arctic ~~sites and~~ regions in ~~Figure 8 agree with observation-based estimates~~the Holocene: 24.1 gC m^{-2} a^{-1} in Fairbanks, Alaska (middle latitude), 5.7–13.1 gC m^{-2} a^{-1} in Alaska (low latitude), 15.6–31.7 gC m^{-2} a^{-1} in West Canada (low latitude), 7.0–30.6 gC m^{-2} a^{-1} in East Canada, 12.9–22.5 gC

m^{-2} a^{-1} in Finland, and 21.9–70.6 in West Siberia ~~(Yu et al. 2008)~~. The simulated results in Figure 8 are reasonably consistent with the field-based values; however, it also shows the need for improvement.

Simulated accumulation rates can ~~be~~show negative ~~while those estimated~~values (corresponding to dissipation or decomposition of stored carbon and the possible release to the atmosphere in gaseous phase). On the contrary, only positive estimates can be reconstructed from excavated cores. Studies show that initiation peaks for northern peatlands occur at approximately 11–9 ka (Yu et al. 2010), and the reported basal age of the core samples from those regions are rarely earlier than 13 ka (Smith et al. 2004, MacDonald et al. 2006, Morris et al. 2018). ~~can only show positive values.~~ The large negative values ~~found in the~~ implying extensive decomposition at approximately 12–13 ka ~~bin are thus worth investigating. Extensive decomposition for this period is~~are consistent with ~~the fact that the basal age derived from the core samples does not go back before 13 ka.~~available information and, thus, are worth further investigation.

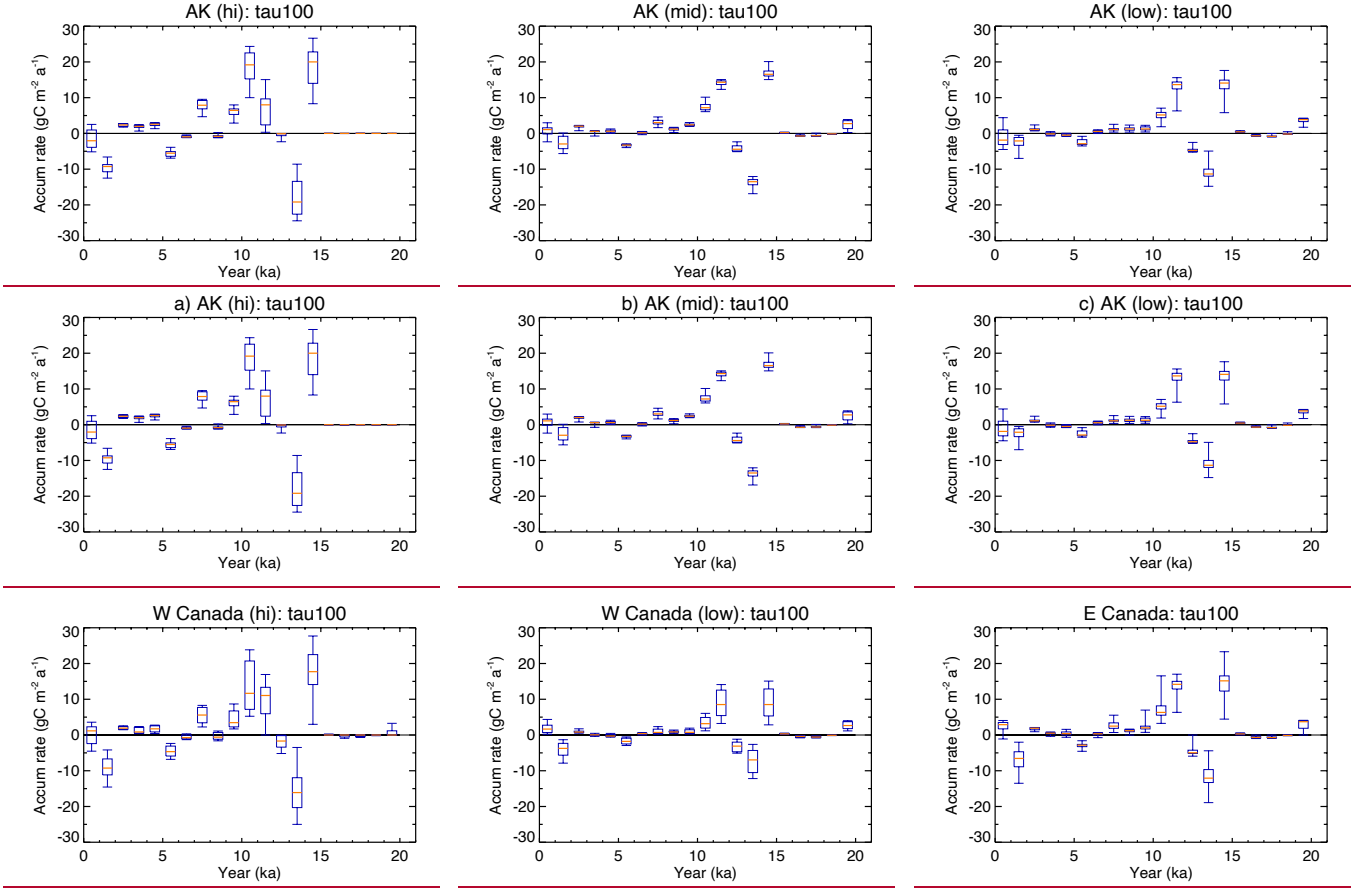

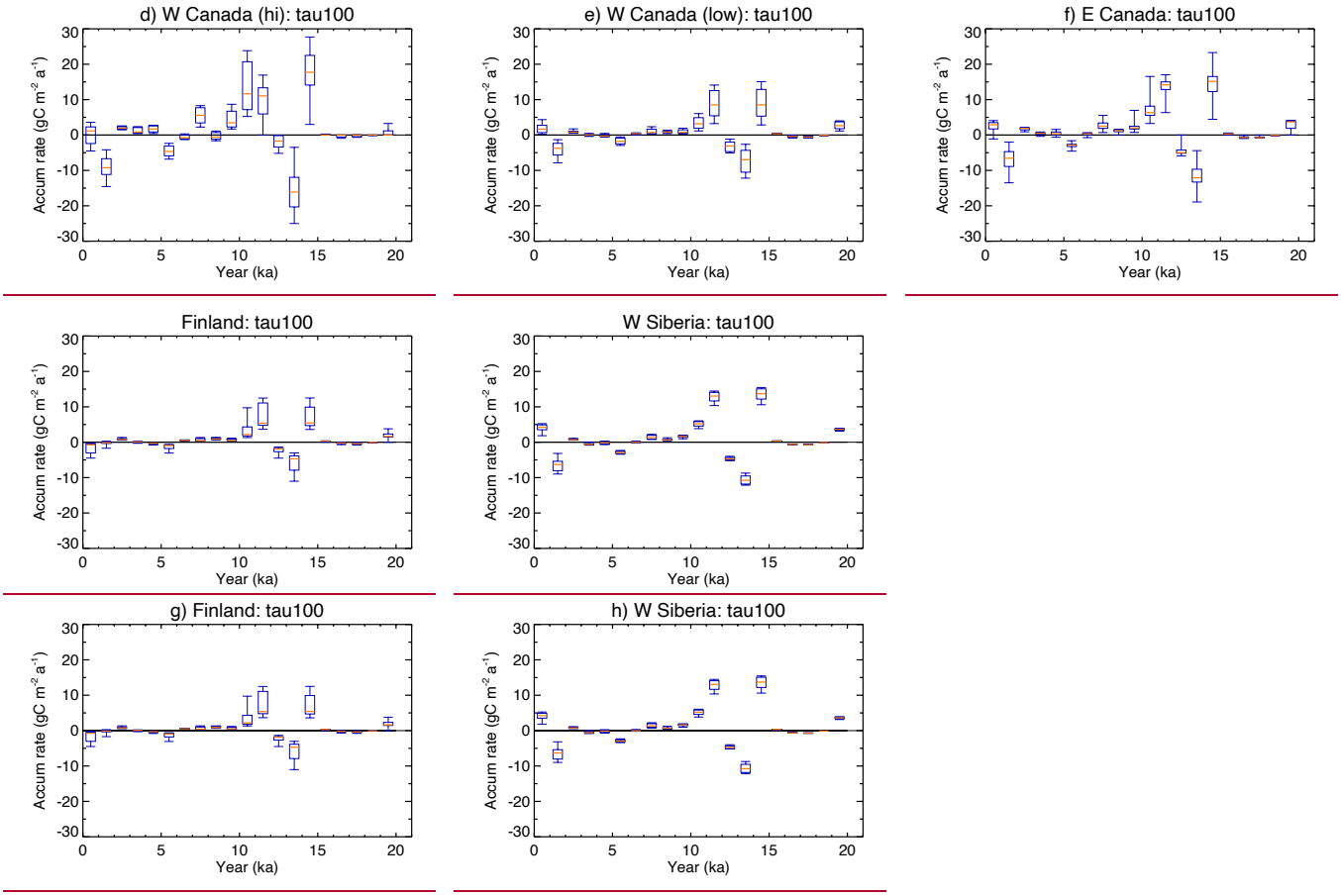

Figure 8: Millennial changes in the carbon accumulation rate (gC m^{-2} a^{-1}) after the LGM for different circum-Arctic regions~~.~~: a) high Alaska, b) mid-Alaska, c) low Alaska, d) high West Canada, e) low West Canada, f) East Canada, g) Finland, and h) West Siberia. The statistical distribution of the accumulation rates, aggregated for each region for each millennial period, is ~~shown~~illustrated by a box-whisker plot. The lowest and highest whiskers of the box-whisker plots show the 10th and 90th percentiles, respectively. The lower and upper edges of the box show the 25th and 75th percentiles, respectively. The 50th percentile (median) is shown by the coloured bar in the box. Areas of each region are shown in Figure 5b.

3.2.3 Changes in ground ice

Similar plots for temporal changes in the regional budget of ICE after the LGM are shown in Fig. 9. In all eight regions, general accumulation of ground ice was ~~observed~~simulated until the end of 15 ka. During the 14–15 ka period, large melting of ground ice occurred in relatively warmer areas, i.e~~.~~, West Canada (low), East Canada, Finland, and West Siberia. The ~~ground ice melted~~melting occurred at 9–11 ka, but at a lower rate. These apparent synchronous melting in these areas at 14–15 ka likely resulted from the single-sourced warming peak of the Bølling-Allerød interstadial in the SeaRISE time series (e.g. Fig. 4a-c) and suggests the need of further studies to include local climate variations to the driving data. Ground ice accumulation continued after 12 ka only in colder regions, such as high-latitude areas in Alaska and West Canada. These

regional differences in and characteristics of simulated ICE evolution suitably correspond ~~well~~ to ~~today's~~current conditions~~, but it is difficult to validate~~; however, the validation of these temporal changes using observation-based sources is difficult.

590

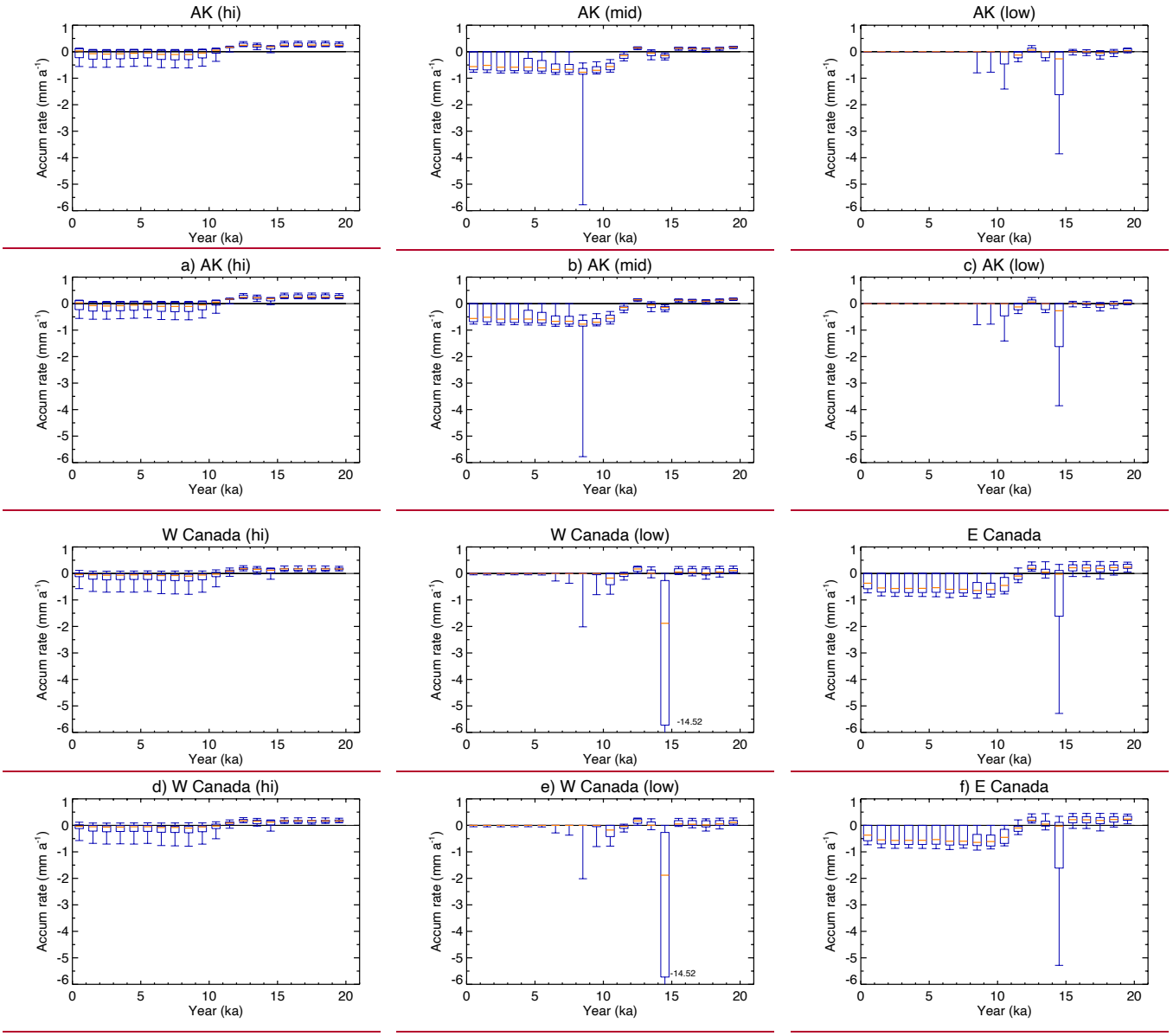

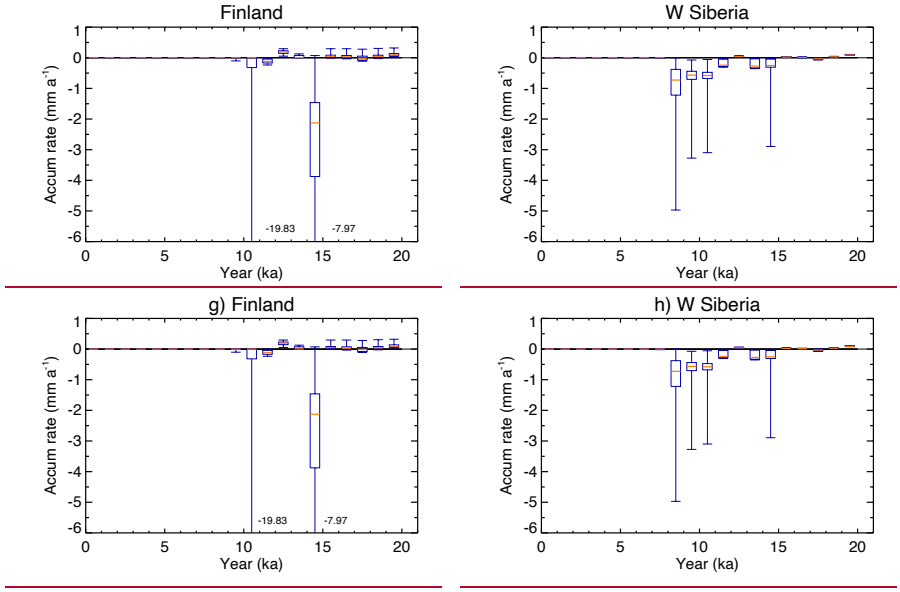

Figure 9: Same as Figure 8, except for ground ice accumulation in mm a^{-1}.

~~4 Discussion~~

~~4.1~~3.3 Implications

3.3.1 Snapshot maps

The simulated time series of SOC, ICE, and soil moisture for each location can be compiled to produce snapshot maps for any period in the last 125 thousand years. ~~In fact, the present-day distributions of simulated SOC and ICE were mapped for the area north of 50°N and presented in an accompanying paper (Saito et al. 2020, under review). In the paper under review,~~the area north of 50°N for any period in the last 125 thousand years, on the annual basis, if the storage capacity allows. Figure 10 exemplifies the SOC and ICE distributions for the LGM (22 ka, the coldest record in the SeaRISE temperature data in the 20–23 ka window) and mid-Holocene (6 ka, the warmest record for the 5–8 ka window) period for $\tau = 100$. A clear and seemingly reasonable contrast between the cold (LGM) and warm (mid-Holocene) climate was observed, although SOC and ICE responded slightly differently. SOC is lower in amount and more contained in extent when the climate was cold, and greater in amount and wider in extent when warm. ICE is wide-spread, but not necessarily greater in amount during the cold environment. In some regions, such as West Siberia, North slope in Alaska, and Canadian High Arctic, ICE appeared to continue accumulating until the initiation of the Holocene (see Fig 6), resulting in the retention of a greater amount of ice under the ground at the mid-Holocene. Note that the SOC and ICE are preserved under the ice sheets (shown by grey dots) until the overlying ice sheets melt (see section 2.3.2).

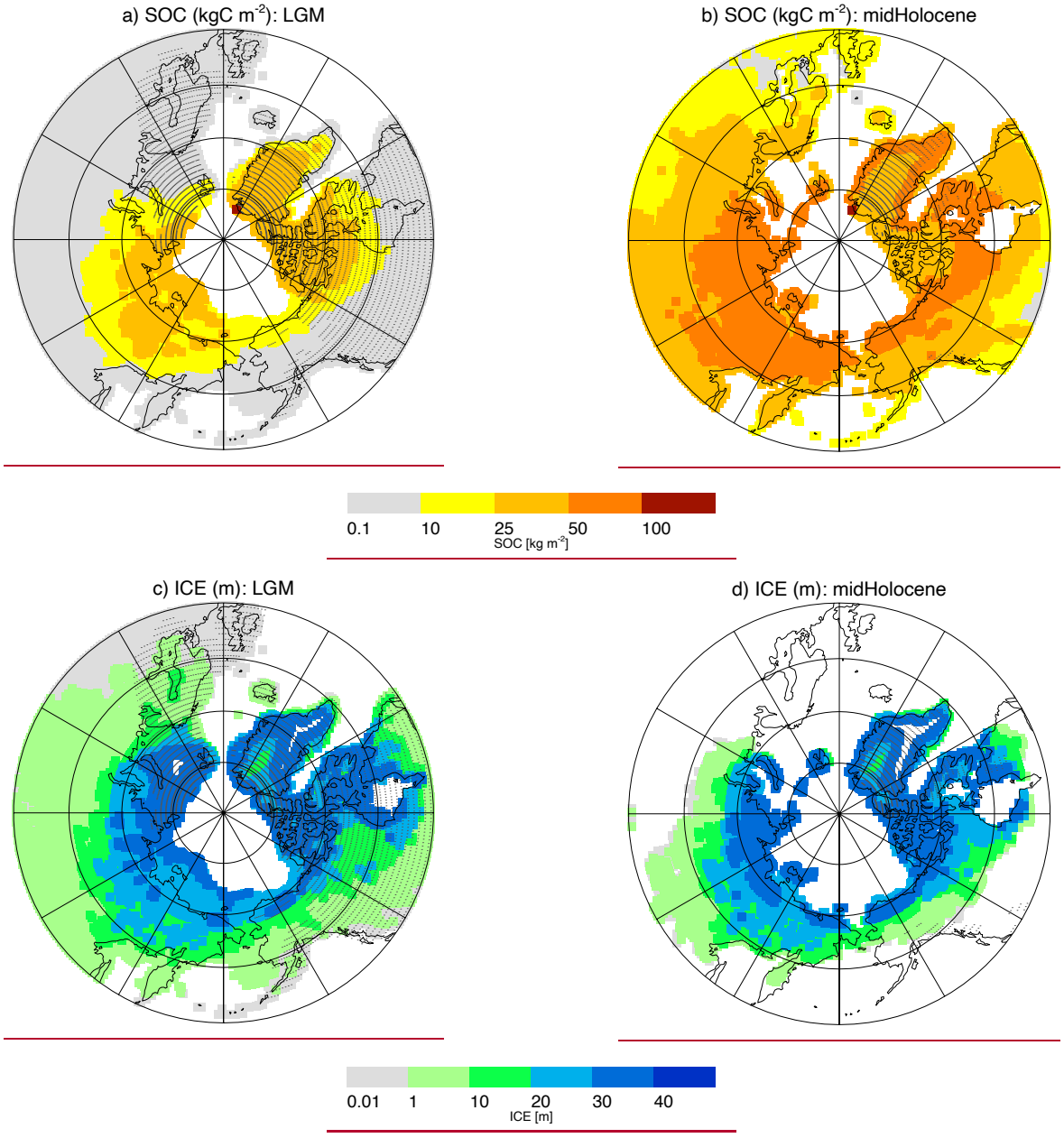

Figure 10: Snapshot maps of soil organic carbon (SOC) and ground ice (ICE) for the periods of the Last Glacial Maximum (LGM, 22ka) and mid-Holocene (6ka). The grey dots show areas of ice sheets and glacial cover.

Another example is the present-day distributions of simulated SOC presented in the accompanying paper (Saito et al. 2020), where we created maps of SOC amounts for each τ at the original 1-degree resolution and discussed differences in and spatial characteristics of simulated distributions for different values of τ. In addition, we developed a ~~methodology to~~

~~associate~~method of associating the value of τ with local topographic-hydrological features derived from a 2 arc-minute digital relief model and produced respective high-resolution circum-Arctic maps of SOC and ICE for comparison with currently available observation-based data (i.e~~,~~, Hugelius et al. 2014, Olefeldt et al. 2016, Brown et al. ~~1997). Similar maps of SOC, ICE, and soil moisture can be produced for different time points (e.g., the Holocene Optimum and the LGM)~~ 1998). These snapshot maps can be used to examine the areal development of variables in the region~~. These snapshot maps can also be used for~~ in the different eras, and to produce initial and/or boundary conditions for Earth System Models (ESMs) or large-scale terrestrial eco-climate models ~~to assess~~in assessing past or present states, or ~~to project~~projecting future impacts on the potential release of GHGs induced by permafrost degradation. Yokohata et al. (2020~~ in review~~) partly used the results derived from the present-day snapshot to quantify the relative impacts resulting from the three pathways described in section 1. Such results can provide localised information on the mechanism of permafrost-related GHG releases (e.g~~,~~, vulnerable areas, potential speed of development) to help stakeholders (i.e~~,~~, policy- and decision-makers, as well as residents at local to global levels) adapt to, stabilize, or mitigate climate change consequences.

~~4~~3.3.2 Future improvements

~~The~~This study shows the simple framework of the modelling concept and the reconstruction ~~methodology~~method of forcing/boundary data creation were useful ~~to reproduce~~ in the reproduction of the evolution and ~~to draw a big picture~~extensive projection of allogenic control, represented by the parameter τ, over long-term carbon dynamics. Nevertheless, there is room for ~~further~~ improvement. ~~Below is a list of possible problems with the current version.~~

The first relates to the forcing data. ~~In order for the resulting reproduction maps to present locality-prone profiles more adequately, the forcing climate data time series need to include information more specific to their history than in this study. Temporal variations in the current method are solely based on a single Greenland ice core. Thence, they are basically in-phase within the simulated circum-Arctic domain, although they incorporate spatial variations such as~~This study employed only one ice core dataset to reconstruct the temperature and precipitation history after the Last Interglacial and used present-day climatology to expand spatially to the circum-Arctic region. Despite a coarse and crude method, (1) it enabled quick preparation of the forcing data; otherwise, relatively more time and effort would be required for compilation from different, sometimes contradicting, ice core data; and (2) it compensated for the lack of time series of spatially-distributed climate data, e.g. outputs from Earth System models, for the entire integration period. This single-core-based dataset successfully produced the first-order approximation of the SOC and ICE evolution in the region that was north of 50°N and demonstrated the model's ability as discussed in sections 3.1 and 3.2. Although the driving time series are basically in-phase within the simulated circum-Arctic domain, we incorporated some aspects of spatial heterogeneity, e.g. variations of topo-geographical changes in coastlines, altitudes, and ice sheets, as well as the meridional gradient on the amplitude of long-term temperature variations (i.e~~,~~, polar amplifications). ~~However~~In reality, however, temporal changes in the general circulations and climate patterns have more distinct regional components (Frenzel et al. 1992, Alley et al. 2002, Nakagawa et al. 2003) and

behaviours at different time scales (Esper et al. 2002, Cook et al. 2004, Mann et al. 2009). As a result, the initiation timings of the Holocene carbon accumulation were ~~heterogeneous globally (Morris et al.~~ globally heterogeneous as demonstrated by Morris et al. (2018), which the current integration scheme failed to account for (section 3.2.1). In the next step, forcing data should be designed to accommodate information that is more specific to the local history so that the resulting time series and maps can reflect regional diversity and characteristics more adequately. ~~2018).~~

The second problem relates to the formulation of carbon dynamics (Eqs. 1–3), hydrology (Eq. 4), and ice dynamics (Eqs. 9–10). With regard to the quantity in the carbon budget, the calculated litter fall tended to be overestimated, as shown in Fig. 6. Equation (1) was designed to express the upper ~~envelope~~envelope of the litter fall for the range of temperatures and precipitation levels considered (i.e~~.~~, -25 °C to 35 °C and 0 mm a^{-1} to 600 mm a^{-1}, Fig. 2). Re-evaluation of ~~the parameter sets~~thermal parameters listed in Table 1 ~~may improve function.~~ is necessary to account for spatial variations in terms of soil types, micro-topography, and geology (sedimentation characteristics). Further, the introduction of a stochastic process to assign a value (e.g~~.~~, between zero and the currently calculated upper value) according to a statistical distribution (e.g~~.~~, uniform or Gaussian) is another possibility. Regarding the quality of the carbon process, the evaluation of the decomposition rate κ, and relatedly, τ may be elaborated (Eqs. 1 and 3). ~~Since~~As one of the primary objectives of this study was to investigate quantitative impacts and functionality of allogenic (external; climatic or environmental conditioning by *Ta*, *Pr* and τ) factors on long-term carbon dynamics, the current model does not specifically consider autogenic (internal, ecosystem-dependent) aspects of the process. However, the examination of the relative contribution of allogenic and autogenic controls on carbon dynamics is important (Lund et al. 2010, van Bellen et al. 2011, Loisel and Yu 2013, Klein et al. 2013, Charman et al. 2015). Possible structure and processes to be incorporated include multiple pools of different soil carbon stability (labile to recalcitrant) for inputs (i.e~~.~~, litter fall) and outputs (i.e~~.~~, rate of decomposition), and their sensitivity to climate and/or hydrology (Boudreau and Ruddick 1991, Hilbert et al. 2000, Biasi et al. ~~2013~~2005).

As for the hydrological modelling, more rigorous examination for the hydrological parameters, γ and ξ (Eq. 4, Table 1), should be performed using updated datasets, e.g. NASA Global Land Data Assimilation System Version 2 (GLDAS-2. Li et al. 2019, 2020) and high-resolution soil database (e.g. SoilGrids250m (Hengl et al. 2017)). Incorporation of lateral flow of water and resolved carbon may be necessary when the model is to be applied to networked grid points in a specific area (e.g. North slope in Alaska, or right bank of the Lena River). Improvement of ice dynamics include a) re-consideration of ground ice behaviour when it is covered by large ice sheets (see section 3.1.2), b) consideration of spatial variability in sediment characteristics (e.g. Canadian shield regions. See also Saito et al. 2020), and vertical profile and physical structure of the subsurface layers for the accumulation of massive ice, and c) spatial and climatic examination of the heat exchange efficiency parameter β (Eq. 10).

The third problem relates to initial values for carbon and water to be specified for the Last Interglacial condition. ~~Since~~As we had no prior information on initial values for that period, we started the integration with a uniform distribution ~~for~~of both soil

carbon and moisture at all grid points north of 50°N. ~~We examined the model's sensitivity to initial values with a small set of different SOC (namely, 5.0, 10.0, 20.0, 22.5, 25.0, 27.5, 30.0, 50.0, and 100.0 kgC m^{-2}) and soil moisture (similarly, 100, 500, 1000, 1500 mm for the 3000 mm column) values in limited locations (cf. Fig 5a). The model sensitivity showed clear dependency on the initial values of SOC but was negligible for soil moisture. Based on this preliminarily examination, we determined the initial values that would produce the most realistic range for the present-day circum-Arctic, namely, 25.0 kgC m^{-2} for SOC and 500 mm for soil moisture.~~ This examination, however, was spatially limited to ~~less than a dozen~~eight locations. ~~It is worth investigating the~~The sensitivity to initial values with larger sets of locations, possibly with a nonuniform distribution (i.e~~.~~, starting with the present-day distribution under the Last Interglacial conditions~~).~~) is worth studying.

5. Conclusion

~~In assessing and projecting the relative risks and impacts of permafrost degradation, the~~The spatial distribution of SOC and ICE provides essential information in the assessment and projection of the risks and impacts of permafrost degradation. However, uncertainties related to geographical distribution and the estimated range of the total amount of stored carbon and ice obtained from synchronic compilations of samples or cores ~~remain large.~~continue to be substantial. We adopted a novel approach to estimate present-day spatial distribution and amounts through diachronic simulations. A ~~conceptual~~ numerical model SOC-ICE-~~01~~v1.0, representing the essential part of the cold-region subsurface carbon and water dynamics by considering frozen ground (permafrost) and land cover changes (ice sheets and coastlines), was developed to calculate the long-term balance of SOC and ICE. The model was integrated for a 125 thousand-year period from the Last Interglacial to the present day for areas north of 50°N to simulate accumulations (or dissipations) of SOC and ICE in the circum-Arctic region. Model performance was evaluated using observation-based data and evidence. Although the model was forced by climate data constructed from a single Greenland ice core, the simulated time series reproduced temporal changes in northern SOC and ICE at different climate locations well and successfully captured circum-Arctic regional differences in characteristics. The model provided useful information for quantitative evaluation of the relative importance of allogenic factors to control soil carbon dynamics under different climatological or topo-geographical conditions.

The set of simulated results can be compiled to produce snapshot maps of the geographical distributions of SOC and ICE in regions north of 50°N. ~~One of these maps was used as the initial or boundary conditions in regional- to global-scale eco-climate models for future projections.~~

Despite its simplicity, the modelling framework employed in this study proved capable of accurately simulating the evolution of the ~~circum-Arctic~~cold-region soil carbon and ground ice, and was powerful enough to provide ~~their present-day~~the spatial distributions~~.~~ in the circum-Arctic. However, some improvements are required in the model, such as the

construction of more locally-specific forcing climate data series, improvement in the structure and parameterization of soil carbon ~~dynamics in terms of inputs and outputs to the subsurface carbon pool~~and ice dynamics, and determination of the initial value distributions for carbon and water integration.

Code and data availability.

The set of model codes, and sample driving and initial/boundary data to run the model are open for research purposes, and provided ~~as supplementary material.~~ at https://github.com/MazaSaito/SOC-ICE/blob/master/SOC_ICE_sample.tar.gz (doi:10.5281/zenode.3839222), which also includes the user manual (https://github.com/MazaSaito/SOC-ICE/blob/master/User_manual.txt), and a sample shell code to run the model.

The open datasets~~, e.g., SeaRISE, ICE-6G_C, GLDAS, CMIP/PMIP, and reanalysis data,~~ used for determining the model parameters, and/or constructing the driving and boundary data are available from the respective data providers~~.~~, i.e., SeaRISE (http://websrv.cs.umt.edu/isis/index.php/SeaRISE_Assessment), ICE-6G_C (https://www.atmosp.physics.utoronto.ca/~peltier/data.php), GLDAS (doi:10.5067/DLVU8VOPKN7L), CMIP5/PMIP3 (available from the ESGF nodes, e.g., https://esgf-node.ipsl.upmc.fr/projects/esgf-ipsl/), and reanalysis data (*UDel_AirT_Precip* at https://www.esrl.noaa.gov/psd/, and ERA-Interim at https://www.ecmwf.int/en/forecasts/datasets/reanalysis-datasets/era-interim).

Author contributions.

KS proposed and managed the overall project, and designed both the study and the model. HM helped with model development and carried out numerical experiments. GI, HO, and TY helped in interpretation and validation of results. All authors read and approved the final manuscript.

Competing interest

The authors declare that they have no competing interests.

Financial support.

This study was conducted as a part of the Environment Research and Technology Development Fund project (2-1605) "Assessing and Projecting Greenhouse Gas Release from Large-scale Permafrost Degradation", supported by the Ministry of Environment and the Environmental Restoration and Conservation Agency.

Acknowledgments

We thank Drs. Atsushi Sato and Hideki Miura for their advice. We also thank Dr. Jun'ichi Okuno for his comments and analysis in interpreting ICE-6G_C data. We are indebted to Drs. Akihiko Ito, Kazuhito Ichii, Hisashi Sato, and Hotaek Park for allowing use of GTMIP Stage 2 simulation data, and to Dr. Taku M. Saitoh for providing 'The compilation data set of ecosystem functions in Asia (version 1.2)'. The *UDel_AirT_Precip* data were provided by the NOAA/OAR/ESRL PSD, Boulder, Colorado, USA, from their Web site at https://www.esrl.noaa.gov/psd/. The professional English language edit was performed by Editage, a division of Cactus Communications.

References

~~Amante, C. and Eakins, B. W.: ETOPO1 1 Arc-Minute Global Relief Model: Procedures, Data Sources and Analysis. In: NOAA Technical Memorandum NESDIS NGDC 24. National Geophysical Data Center, NOAA. doi:10.7289/V5C8276M, 2009. Accessed 23 Dec 2019~~

AMAP: Snow, Water, Ice and Permafrost in the Arctic (SWIPA): Climate Change and the Cryosphere. Arctic Monitoring and Assessment Programme (AMAP), Oslo, Norway, 2011.

AMAP: Snow, Water, Ice and Permafrost in the Arctic (SWIPA) 2017. Arctic Monitoring and Assessment Programme (AMAP), Oslo, Norway, 2017.

Argus, D. F., Peltier, W. R., Drummond, R., and Moore, A. W.: The Antarctica component of postglacial rebound model ICE-6G_C (VM5a) based upon GPS positioning, exposure age dating of ice thicknesses, and relative sea level histories. Geophys. J. Int. 198(1):537-563, doi:10.1093/gji/ggu140, 2014.

Beilman, D. W., MacDonald, G. M., Smith, L. C., and Reimer, P. J.: Carbon accumulation in peatlands of West Siberia over the last 2000 years. Gloval Biogeochemical Cycles 23, GB1012, doi:10.1029/2007GB003112, 2009.

Belyea, L. R., and Baird, A. J.: Beyond "The limits to peat bog growth": Cross-scale feedback in peatland development. Ecological Monographs, 76(3), ,299–322, 2006.

Biasi, C., Rusalimova, O., Meyer, H., Kaiser, C., Wanek, W., Barsukov, P., Junger, H. and Richter, A.: Temperature-dependent shift from labile to recalcitrant carbon sources of arctic heterotrophs. Rapid Communications in Mass Spectrometry, 19 (11), 1401-1408. Doi: 10.1002/rcm.1911, 2005.

Bindshadler, R. A., Nowicki, S., Abe-Ouchi, A., Aschwanden, A., Choi, H., Fastook, J., Granzow, G., Greve, R., Gutowski, G., Herzfeld, U., Jackson, C., Johnson, J., Khroulev, C., Levermann, A., Lipscomp, W. H., Martin, M. A., Morlighem, M., Parizek, B. R., Pollard, D., Price, S. F., Ren, D., Saito, F., Sato, T., Seddik, H., Seroussi, H., Takahashi, K., Walker, R., Wang, W. L.: Ice-sheet model sensitivities to environmental forcing and their use in projecting future sea level (the SeaRISE project). Journal of Glaciology 59(214) doi:10.3189/2013JoG12J125, 2013.

Boudreau, B. P. and Ruddick, B. R.: On a reactive continuum representation of organic matter diagenesis. American Journal of Science, 291, 507-538, 1991.

Braconnot, P., Harrison, S. P., Kageyama, M., Bartlein, P. J., Masson-Delmotte, V., Abe-Ouchi, A., Otto-Bliesner, B., Zhao, Y.: Evaluation of climate models using palaeoclimatic data. Nature Climate Change 2:417–424. doi:10.1038/NCLIMATE1456, 2012.

~~Bradley, R. S.: Paleoclimatology: Reconstructing climates of the Quaternary. Second edition Academic Press, San Diego, 1999..~~

Brown, J., Ferrians, O. J., Heginbottom, J. A., and Melnikov, E. S.: Circum-arctic map of permafrost and ground ice conditions. National Snow and Ice Data Center, Digital media, Boulder, CO, ~~1997~~1998 (revised 2002).

Brouchkov, A., and Fukuda, M.: Preliminary Measurements on Methane Content in Permafrost, Central Yakutia, and some Experimental Data. Permafrost Periglac. Process. 13: 187–197, 2002.

Charman, D. J., Amesbury, M. J., Hinchliffe, W., Hughes, P. D. M., Mallon, G., Blake, W. H., Daley, T. J., Gallego-Sala, A. V., and Mauquoy, D.: Drivers of Holocene peatland carbon accumulation across a climate gradient in northeastern North America. Quaternary Science Reviews 121:110-119, 2015.

Clymo, R. S.: The limits to peat bog growth. Philosophical Transactions of the Royal Society of London B 303:605–654, 1984.

Clymo, R. S.: Models of peat growth. Suo 43:127–136, 1992.

Conant, R., Ryan, M., Ågren, G. I., Birgé, H., Davidson, E., Eliasson, P., Evans, S., Frey, S., Giardina, Ch., Hopkins, F., Hyvönen, R., Kirschbaum, M., Lavallee, J., Leifeld, J., Parton, W., Steinweg, J. M., Wallenstein, M., Wetterstedt, M., Bradford, M.: Temperature and soil organic matter decomposition rates – synthesis of current knowledge and a way forward. Global Change Biology. 17. 3392 - 3404. 10.1111/j.1365-2486.2011.02496.x, 2011.

De Deyn, G. B., Cornelissen, J. H. C. and Bardgett, R. D.:. Plant functional traits and soil carbon sequestrationin contrasting biomes, Ecology Letters, 11, 516–531, doi: 10.1111/j.1461-0248.2008.01164.x, 2008.

Dean, J. F., van derVelde, Y., Garnett, M. H., Dinsmore, K. J., Baxter, R., Lessels, J. S., Smith, P., Street, L. E.: Abundant pre-industrial carbon detected in Canadian Arctic headwaters: implications for the permafrost carbon feedback. Environ. Res. Lett. 13, 034024, 2018a.

Dean, J. F., Middelburg, J. J., Röckmann, T., Aerts, R., Blauw, L. G., Egger, M., Jetten, M. S. M., de Jong, A. E. E., Meisel, O. H., Rasigraf, O., Slomp, C. P., in't Zandt, M. H., and Dolman, A. J.: Methane Feedbacks to the Global Climate System in a Warmer World. Reviews of Geophysics, 56:207–250, doi:10.1002/2017RG000559, 2018b.

Dee, D. P., Uppala, S. M., Simmons, A. J., Berrisford, P., Poli, P., Kobayashi, S., Andrae, U., Balmaseda, M. A., Balsamo, G., Bauer, P., Bechtold, P., Beljaars, A. C. M., van de Berg, L., Bidlot, J., Bormann Delsol, C., Dragani, R., Fuentes, M., Geer, A. J., Haimberger, L., Healy, S. B., Hersbach, H., Hólm, E. V., Isaksen, L., Kållberg, P., Köhler, M., Matricardi, M., McNally, A. P., Monge-Sanz, B. M. , Morcrette, J. J., Park, B. K., Peubey, C., de Rosnay, P., Tavolato, C., Thépaut, J. N., and Vitart, F.: The ERA-Interim reanalysis: configuration and performance of the data assimilation system. Q. J. Roy. Meteor. Soc., 137:553–597, 2011.

Dufresne, J. L., Foujols, M. A., Denvil, S. et al. :. Climate change projections using the IPSL-CM5 Earth System Model: from CMIP3 to CMIP5. Clim Dyn (2013) 40: 2123. https://doi.org/10.1007/s00382-012-1636-1, 2013.

Dyke, A. S.: Late Quaternary Vegetation History of Northern North America Based on Pollen Macrofossil, and Faunal Remains. Géographie physique et Quaternaire 59(2-3):211-262, 2005.

French, H. M.: The periglacial environment. John Wiley & Sons Ltd., Chichester, England, pp. 458, 2007.

Frenzel, B., Pécsi, M., and Velichko, A. A. (Eds.): Atlas of Paleoclimates and Paleoenvironments of the Northern Hemisphere, Geographical Research Institute, Hungarian Academy of Sciences, Budapest, 153 pp., Gustav Fischer Verlag, Stuttgart, 1992.

Gent, P.R., Danabasoglu, G., Donner, L.J., Holland, M.M., Hunke, E.C., Jayne, S.R., Lawrence, D.M., Neale, R.B., Rasch, P.J., Vertenstein, M., Worley, P.H., Yang, Z., and Zhang, M.: The Community Climate System Model Version 4. J. Clim. 24, 4973-4991, 2011.

Gido, N. A. A., Bagherbandi, M., Sjöberg, L. E., and Tenze, R.: Studying permafrost by integrating satellite and in situ data in the northern high-latitude regions. Acta Geophysica 67:721–734 doi:10.1007/s11600-019-00276-4, 2019.

Gorham, E. Northern Peatlands: Role in the carbon cycle and probable responses to climatic warming. Ecol. Appl. 1, 182–195, 1991.

Hengl, T., Mendes de Jesus, J., Heuvelink, G. B. M., Ruiperez Gonzalez, M., Kilibarda, M., Blagotić, A., Shangguan, W., Wright, M. N., Geng, X., Bauer-Marschallinger, B., Guevara, M. A., Vargas, R., MacMillan, R. A., Batjes, N. H., Leenaars, J. G. B., Ribeiro, E., Wheeler, I., Mantel, S., and Kempen, B.: SoilGrids250m: Global gridded soil information based on machine learning, PLoS ONE, 12, e0169748, https://doi.org/10.1371/journal.pone.0169748, 2017.

Harden, J. W., Sundquist, E. T., Stallard, R. F., and Mark, R. K.: Dynamics of Soil Carbon During Deglaciation of the Laurentide Ice Sheet. Science. 258, 5090, 1921-1924, 1992.

Hilbert, D. W., Roulet, N., and Moore, T.: Modelling and analysis of peatlands as dynamical systems. Journal of Ecology, 88, 230-242, 2000.

Hu, F., Philip, S., Higuera, E., Duffy, P., Chipman, M. L., Rocha, A. V., Young, A. M., Kelly, R., and Dietze, M. C.: Arctic tundra fires: natural variability and responses to climate change. Front Ecol Environ 2015; 13(7): 369–377, doi:10.1890/150063, 2015.

Hugelius, G., Tarnocai, C., Broll, G., Canadell, J. G., Kuhry, P., and Swanson, D. K.: The Northern Circumpolar Soil Carbon Database: spatially distributed datasets of soil coverage and soil carbon storage in the northern permafrost regions. Earth Syst. Sci. Data, 5:3–13, 2013.

Hugelius, G., Strauss, J., Zubrzycki, S., Harden, J. W., Schuur, E. A. G., Ping, C. L., Schirrmeister, L., Grosse, G., Michaelson, G. J., Koven, C. D., O'Donnell, J. A., Elberling, B., Mishra, U., Camill, P., Yu, Z., Palmtag, Kuhry, P.: Estimated stocks of circumpolar permafrost carbon with quantified uncertainty ranges and identified data gaps. Biogeosciences 11(23):6573-6593, 2014.

Hugelius, G., Loisel, J., Chadburn, S., Jackson, R. B., Jones, M., MacDonald, G., Marushchak, M., Olefeldt, D., Packalen, M., Siewert, M. B., Treat, C., Turetsky, M., Voigt, C., and Yu, Z.: Large stocks of peatland carbon and nitrogen are vulnerable to permafrost thaw. Proceedings of the National Academy of Sciences, 117 (34):20438-20446, 2020.

Ingram, H. A. P.: Soil layers in mires: function and terminology. Journal of Soil Science 29:224–227, 1978.

IPCC: Climate Change 2013: The Physical Science Basis. Contribution of Working Group I to the Fifth Assessment Report of the Intergovernmental Panel on Climate Change [Stocker, T.F., Qin, D., Plattner, G.-K., Tignor, M., Allen, S.K., Boschung, J., Nauels, A., Xia, Y., Bex, V., and Midgley, P. M. (eds.)]. Cambridge University Press, Cambridge, United Kingdom and New York, NY, USA, 2013.

Ito, A.: Methane emission from pan-Arctic natural wetlands estimated using a process-based model, 1901–2016. Polar Science 21: 26–36. DOI: 10.1016/j.polar.2018.12.001, 2019.

Iwahana, G., Uchida, M., Liu, L., Gong, W., Meyer, F., Guritz, R., Yamanokuchi, T., and Hinzman, L.: InSAR Detection and Field Evidence for Thermokarst after a Tundra Wildfire, Using ALOS-PALSAR. Remote Sensing, 8(3), 218, 2016.

Jassey, V. E., and Signarbieux, J., C.: Effects of climate warming on Sphagnum photosynthesis in peatlands depend on peat moisture and species-specific anatomical traits. Glob Change Biol. 25:3859–3870. DOI: 10.1111/gcb.14788, 2019.

Jenny, H., Gessel, S. P., and Bingham, F. T.: Comparative study of decomposition rates of organic matter in temperate and tropical regions. Soil Science 68:419–432, 1949.

Johnsen, S., Clausen, H., Dansgaard, W. et al. Irregular glacial interstadials recorded in a new Greenland ice core. Nature 359, 311–313, doi: 10.1038/359311a0, 1992.

Johnsen, S. J., Clausen, H. B., Dansgaard, W., Gundestrup, N. S., Hammer, C. U., Andersen, U., Andersen, K. K., Hvidberg, C. S, Dahl-Jensen, D., Steffensen, J. P., Shoji, H., Sveinbjörnsdóttir, Á. E., White, J., Jouzel, J., and Fisher, D.: The δ18O record along the Greenland Ice Core Project deep ice core and the problem of possible Eemian climatic instability. JGR, 102, 26397-26410, doi:10.1029/97JC00167, 1997.

Jones, B. M., Kolden, C.A., Jandt, R., Abatzoglou, J.T., Urban, F. and Arp, C.D.: Fire behavior, weather, and burn severity of the 2007 Anaktuvuk River tundra fire, North Slope, Alaska. Arctic, Antarctic and Alpine Research, 41:309-316, 2009.

Jones, M. C. and Yu, Z.:, Rapid deglacial and early Holocene expansion of peatlands in Alaska. PNAS, 107 (16), 7347–7352. Doi: 10.1073/pnas.0911387107, 2010.

Jorgenson, M. T., Kanevskiy, M., Shur, Y., Moskalenko, N., Brown, D. R. N., Wickland, K., Striegl, R., and Koch, J.: Role of ground ice dynamics and ecological feedbacks in recent ice wedge degradation and stabilization, J. Geophys. Res. Earth Surf., 120, 2280–2297, doi:10.1002/2015JF003602, 2015.

Kanevskiy, M., Shur Y, Fortier D, Jorgenson MT, and Stephani E.: Cryostratigraphy of late Pleistocene syngenetic permafrost (yedoma) in northern Alaska, Itkillik River exposure, Quaternary Research 75: 584–596. DOI:10.1016/j.yqres.2010.12.003, 2011.

Kanevskiy, M., Shur, Y., Jorgenson, M. T., Ping, C. L., Michaelson, G. J., Fortier, D., et al.: Ground ice in the upper permafrost of the Beaufort Sea coast of Alaska. Cold Regions Science and Technology, 85, 56–70. doi:10.1016/j.coldregions.2012.08.002, 2013.

Kaplan, J. O., Bigelow, N. H., Prentice, I. C., Harrison, S. P., Bartlein, P. J., Christensen, T. R., Cramer, W., Matveyeva, N. V., McGuire, A. D., Murray, D. F., Razzhivin, V. Y., Smith, B., Walker, D. A., Anderson, P. M., Andreev, A. A., Brubaker, L. B., Edwards, M. E., and Lozhkin, A. V.: Climate change and Arctic ecosystems: 2. Modeling, paleo-model comparisons, and future projections. J. Geophys. Res. 108, doi: 10.1029/2002D002559, 2003.

Klein, E. S., Booth, R. K., Yu, Z., Mark, B. G., and Stansell, N. D.: Hydrology-mediated differential response of carbon accumulation to late Holocene climate change at two peatlands in Southcentral Alaska. Quaternary Science Reviews, 64, 61-75, 2013.

Koven, C. D., Schuur, E. A. G., Schädel, C., Bohn, T. J., Burke, E. J., Chen, G., Chen, X,. Ciais, P., Grosse, G., Harden, J. W., Hayes, D. J., Hugelius, G., Jafarov, E. E., Krinner, G., Kuhry, P., Lawrence, D. M., MacDougall, A. H., Marchenko, S. S., McGuire, A. D., Natali, S. M., Nicolsky, D. J., Olefeldt, D., Peng, S., Romanovsky, V. E., Schaefer, K. M., Strauss, J., Treat, C. C., and Turetsky, M.: A simplified, data-constrained approach to estimate the permafrost carbon–climate feedback. Phil. Trans. R. Soc. A Math. Phys. Eng. Sci. 373, 20140423, 2015.Kukla, G. J., Bender, M. L., de Beaulieu, J.-L., Bond, G., Broecker, W. S., Cleveringa, P., Gavin, J. E., Herbert, T. D., Imbrie, J., Jouzel, J., Keigwin, L. D., Knudsen, K.-L., McManus, J. F., Merkt, J., Muhs, D. R., Müller, H., Poore, R. Z., Porter, S. C, Seret, G., Shackleton, N. J., Turner, C., Polychronis C., Tzedakis, C., and Winograd, I. J.: . Last Interglacial Climates. Quaternary Research 58, 2–13. doi:10.1006/qres.2001.2316, 2002.

Lenton, T. M.: Arctic climate tipping points. Ambio 41(1): 10-22. doi:10.1007/s13280-011-0221-x, 2012.

Loisel, J., van Bellen, S., Pelletier, L., Talbot, J., Hugelius, G., Karran, D., Yu, Z., Nichols, J., and Holmquist, J.: Insights and issues with estimating northern peatland carbon stocks and fluxes since the Last Glacial Maximum. Earth-Science Reviews 165:59–80, 2017.

Loisel, J., and Yu, Z.: Holocene peatland carbon dynamics in Patagonia. Quaternary Science Reviews 69, 125-141, 2013.

Luo, Zh., Wang, G., and Wang, E.: Global subsoil organic carbon turnover times dominantly controlled by soil properties rather than climate. Nature Communications, 10:3688, doi: 10.1038/s41467-019-11597-9, 2019.

Jorgenson, M. T., Kanevskiy, M., Shur, Y., Moskalenko, N, . Brown, D.R.N., Wickland, K., Striegl, R., and Koch, J.: Role ofground ice dynamics and ecological feed-backs in recent ice wedge degradation and stabilization. J. Geophys. Res. Earth Surf.,120:2280–2297, doi:10.1002/2015JF003602, 2015.

Li, B., Beaudoing, H., and Rodell, M.: GLDAS Catchment Land Surface Model L4 daily 0.25 x 0.25 degree GRACE-DA1 V2.2, Greenbelt, Maryland, USA, Goddard Earth Sciences Data and Information Services Center (GES DISC), Accessed: [Data Accessed on October 28, 2020], 10.5067/TXBMLX370XX8, 2020.

Li, B., Rodell, M., Kumar, S., Beaudoing, H., Getirana, A., Zaitchik, B. F., de Goncalves, L. G., Cossetin, C., Bhanja, S., Mukherjee, A., Tian, S., Tangdamrongsub, N., Long, D., Nanteza, J., Lee, J., Policelli, F., Goni, I. B., Daira, D., Bila, M.,

de Lannoy, G., Mocko, D., Steele-Dunne, S. C., Save, H., Bettadpuret, S.: Global GRACE data assimilation for groundwater and drought monitoring: Advances and challenges. Water Resources Research, 55:7564-7586. doi:10.1029/2018wr024618, 2019.

Lunardini, V.: Permafrost formation time, CRREL Report 95-8, 1995.

Lund M., Lafleur, P. M., Roulet,N. T., Lindroth, A., Christensen, T. R., Aurela, M., Chojnicki, B. H., Flanagan, L. B., Humphreys, E. R., Laurila, T., Oechel, W. C., Olejnik, J., Rinne, J., Schubert, P. and Nilson, M. B.:. Variability in exchange of CO2 across 12 northern peatland and tundra sites. Global Change Biology, 16, 2436–2448, doi: 10.1111/j.1365-2486.2009.02104.x, 2010.

MacDonald, G. M., Beilman, D. W., Kremenetski, K. V., Sheng, Y., Smith, L. C., and Velichko, A. A.: Rapid Early Development of Circumarctic Peatlands and Atmospheric CH4 and CO2 Variations. Science 314:285-288, doi:10.1126/science.1131722, 2006.

MacDougall, A. H. and Knutti, R.: Projecting the release of carbon from permafrost soils using a perturbed parameter ensemble modelling approach. Biogeosciences, 13;2123–2136. doi:10.5194/bg-13-2123-2016, 2016.

McGuire, A.D., Koven, C., Lawrence, D.M., Clein, J.S., Xia, J., Beer, C., Burke, E., Chen, G., Chen, X., Delire, C., Jafarov, E., MacDougall, A.H., Marchenko, S., Nicolsky, D., Peng, S., Rinke, A., Saito, K., Zhang, W., Alkama, R., Bohn, T.J., Ciais, P., Decharme, B., Ekici, A., Gouttevin, I., Hajima, T., Hayes, D.J., Ji, D., Krinner, G., Lettenmaier, D. P., Miller, P.A., Moore, J.C., Romanovsky, V., Schadel, C., Schaefer, K., Schuur, E.A.G., Smith, B., Sueyoshi, T., and Zhuang, Q.: Variability in the sensitivity among model simulations of permafrost and carbon dynamics in the permafrost region between 1960 and 2009. Global Biogeochemical Cycles, 30:1015-1037, 2016.

Miyazaki, S., Saito, K., Mori, J., Yamazaki, T., Ise, T., Arakida, H., Hajima, T., Iijima, Y., Machiya, H., Sueyoshi, T., Yabuki, H., Burke, E. J., Hosaka, M., Ichii, K., Ikawa, H., Ito, A., Kotani, A., Matsuura, Y., Niwano, M., Nitta, T., O'ishi, R., Ohta, T., Park, H., Sasai, T., Sato, A., Sato, H., Sugimoto, A., Suzuki, R., Tanaka, K., Yamaguchi, S., and Yoshimura, K.: The GRENE-TEA model intercomparison project (GTMIP): overview and experiment protocol for Stage 1, Geosci. Model Dev., 8, 2841–2856, doi:10.5194/gmd-8-2841-2015, 2015.

Morris, P. J., Swindles, G. T., Valdes, P. J., Ivanovic, R. F., Gregoire, L. J., Smith, M. W., Tarasov, L., Haywood, A. M., and Bacon, K. L.: Global peatland initiation driven by regionally asynchronous warming. PNAS, 115 (19), 4851–4856. doi:10.1073/pnas.1717838115, 2018.

Murton, J. B., Goslar, T., Edwards, M. E., Bateman, M. D., Danilov, P. P., Savvinov, G. N., Gubin, S. V., Ghaleb, B., Haile, J., Kanevskiy, M., Lozhkin, A. V., Lupachev, A. V., Murton, D. K., Shur, Y., Tikhonov, A., Vasil'chuk, A. C., Vasil'chuk, Y. K., and Wolfe, S. A.: Palaeoenvironmental interpretation of Yedoma silt (Ice Complex) deposition as cold-climate loess, Duvanny Yar, Northeast Siberia. Permafr. Periglac. Process. 26(3):208–288. doi:10.1002/ppp.1843, 2015.

Muskett, R. R., and Romanovsky, V. E.: Alaskan permafrost groundwater storage changes derived from grace and ground measurements. Remote Sens 3:378–397. doi:10.3390/rs302 0378, 2011.

Narita, K., Harada, K., Saito, K., Sawada, Y., Fukuda, M. and Tsuyuzaki, Sh.: Vegetation and permafrost thaw depth 10 years after a tundra fire in 2002, Seward Peninsula, Alaska. Arctic, Antarctic, and Alpine Research, 47 (3), 547–559, doi:10.1657/AAAR0013-031, 2015.

Nichols, J. E., and Peteet, D. M.: Rapid expansion of northern peatlands and doubled estimate of carbon storage. Nature Geoscience, 12: 917–921, doi: 10.1038/s41561-019-0454-z, 2019.

Olefeldt, D., Goswami, S., Grosse, G., Hayes, D., Hugelius, G., Kuhry, P., McGuire, A. D., Romanovsky, V. E., Sannel, A. B. K., Schuur, E. A. G., and Turetsky, M. R.: Circumpolar distribution and carbon storage of thermokarst landscapes. Nature Comm. 7, 13043, doi:10.1038/ncomms13043, 2016.

Park, H., Iijima, Y., Yabuki, H., Ohta, T., Walsh, J., Kodama, Y. andOhata, T.: The application of a coupled hydrological and biogeochemical model (CHANGE) for modeling of energy, water, and CO2 exchanges over a larch forest in eastern Siberia. J. Geophys. Res., 116, D15102, doi：10.1029/2010JD015386, 2011.

Peltier, W. R., Argus, D. F., and Drummond, R.: Space geodesy constrains ice-age terminal deglaciation: The global ICE-6G_C (VM5a) model. Geophys. Res. Solid Earth, 120, 450-487, doi:10.1002/2014JB011176, 2015.

Perruchoud, D., Joos, F., Fischlin, A., Hajdas, I., and Bonani, G.: Evaluating timescales of carbon turnover in temperate forest soils with radiocarbon data. Global Biogeochemical Cycles, 13(2), 555-573,1999.

Plaza, C., Pegoraro, E., Bracho, R., Kathryn, G. C., Crummer, G., Hutchings, J. A., Hicks Pries, C. E., Mauritz, M., Natali, S. M., Salmon, V. G., Schädel, C., Webb, E. E., and Schuur, E. A. G.: Nature Geoscience 12: 627–631. doi:10.1038/s41561-019-0387-6, 2019.

Prentice, I. C., Guiot, J., Huntley, B., Jolly, D., and Cheddadi, R.: Reconstructing biomes from palaeoecological data: A general method and its application to European pollen data at 0 and 6 ka. Climate Dynamics 12, 185-194, 1996.

Pugh T.A.M. et al. Understanding the uncertainty in global forest carbon turnover. Biogeosciences Discussions, doi:10.5194/bg-2019-491, 2020.

Rodell, M. and Beaudoing, H. K: GLDAS Mosaic Land Surface Model L4 3 Hourly 1.0 x 1.0 degree Subsetted V001, Greenbelt, Maryland, USA, Goddard Earth Sciences Data and Information Services Center (GES DISC), doi:10.5067/DLVU8VOPKN7L, 2007. Accessed: January 22, 2020.

Rodell, M., Houser, P.R., Jambor, U., Gottschalck, J., Mitchell, K., Meng, C., Arsenault, K., Cosgrove, B., Radakovich, J., Bosilovich, M., Entin, J. K., Walker, J.P., Lohmann, D., and Toll, D.: The Global Land Data Assimilation System, Bull. Amer. Meteor. Soc., 85, 381-394, doi:10.1175/BAMS-85-3-381, 2004.

Saito, K., Marchenko, S., Romanovsky, V., Hendricks, A., Bigelow, N., Yoshikawa, K., and Walsh, J.: Evaluation of LPM permafrost distribution in NE Asia reconstructed and downscaled from GCM simulations. Boreas, 43, 733–749. doi:10.1111/bor.12038, 2014.

Saito, K., Trombotto Liaudat, D., Yoshikawa, K., Mori, J., Sone, T., Marchenko, S., Romanovsky, V., Walsh, J., Hendricks, A., and Bottegal, E.: Late Quaternary Permafrost Distributions Downscaled for South America: Examinations of GCM-based Maps with Observations. Permafrost and Periglacial Processes, 27: 43–55, 2016.

Saito, K., Machiya, H., Iwahana, G., Ohno, H., and Yokohata, T.: Mapping circum-Arctic organic carbon, ground ice, and vulnerability of ice-rich permafrost to degradation. In review at Progress in Earth and Planetary Science, 2020.

Sannel, A. B. K., and Kuhry, P.: Warming-induced destabilization of peat plateau/thermokarst lake complexes, J. Geophys. Res., 116, G03035, doi:10.1029/2010JG001635, 2011.

Sato, H., Kobayashi, H., Iwahana, G. and Ohta, T.: Endurance of larch forest ecosystems in eastern Siberia under warming trends. Ecol. Evol., 6, 5690-5704, 2016.

Schaefer, K., Lantuit, H., Romanovsky, V. E., Schuur, E. A. G., and Witt, R.: The impact of the permafrost carbon feedback onglobal climate. Environ. Res. Lett. 9 085003, 2014.

Schneider von Deimling, T., Grosse, G., Strauss, J., Boike, J., Schirrmeister, L., Morgenstern, A., Schaphoff, S. and Meinshausen, M.: Observation-based modelling of permafrost carbon fluxes with accounting for deep carbon deposits and thermokarst activity. Biogeosciences, 12, 3469–3488, 2015.

Schuur, E. A. G., Abbott, B., and Permafrost Carbon Network: Permafrost Carbon High risk of permafrost thaw. Nature 480(7375):32-33, 2011. Smith, L. C., MacDonald, G. M., Velichko, A. A., Beilman, D. W. Borisova, O. K. Frey, K. E., Kremenetski, K. V., and Shen Y.: Siberian Peatlands a Net Carbon Sink and Global Methane Source Since the Early Holocene. Science, 303, 2004.

Strauss, J., Schirrmeister, L., Grosse, G., Fortier, D., Hugelius, G., Knoblauch, C., Romanovsky, V., Schädel, C., Schneidervon Deimling, T., Schuur, E. A. G., Shmelev, D., Ulrich, M., and Veremeeva, A.: Deep Yedoma permafrost: A synthesis of depositional characteristics and carbon vulnerability. Earth-Science Reviews 172:75–86. doi:10.1016/j.earscirev.2017.07.007, 2017.

Stroeven, A. P., Hättestrand, C., Kleman, J., Heyman, J., Fabel, D., Fredind, O., Goodfellow, B. W., Harbor, J. M., Jansen, J. D., Olsen, L., Caffee, M. W., Fink, D., Lundqvist, J., Rosqvist, G. C., Strömberg, B., and Jansson, K. N.: Deglaciation of Fennoscandia. Quaternary Science Reviews 147: 91-121, doi:10.1016/j.quascirev.2015.09.016, 2016.

Sueyoshi, T., Saito, K., Miyazaki, S., Mori, J., Ise, T., Arakida, H., Suzuki, R., Sato, A., Iijima, Y., Yabuki, H., Ikawa, H., Ohta, T., Kotani, A., Hajima, T., Sato, H., Yamazaki, T., and Sugimoto, A.: The GRENE-TEA Model Intercomparison Project (GTMIP) stage 1 forcing dataset, *Earth Syst. Sci. Data*, 8, 1-14, doi:10.5194/essd-8-1-2016, 2016.

Svenning, J.-C., and Sandel, B.: Disequilibrium vegetation dynamics under future climate change. Am. J. Bot. 100, 1266–1286, doi:10.3732/ajb.1200469, 2013.

~~Tarboton, D. G.: Terrain Analysis Using Digital Elevation Models (TauDEM). Available via Hydrologi Research Group, Utah State University, 1989. http://hydrology.usu.edu/taudem/taudem5/. Accessed 23 Dec 2019~~

Taylor, K. E., Stouffer, R. J. and Meehl, G. A.: An overview ofcmip5 and the experiment designBull. Am. Meteorol. Soc.93485–98, 2012.

Thornton, P.E., Law, B.E., Gholz, H. L., Clark, K.L., Falge, E., Ellsworth, D. S., Goldstein, A.H., Monson, R. K., Hallinger, D., Falk, M., Chen, J. and Sparks, J. P.: Modeling and measuring the effects of disturbance history and climate on carbon and water budgets in evergreen needleleaf forests. Agric. For Meteorol., 113, 185-222, 2002.

Turetsky, M. R., Abbott, B. W., Jones, M. C, Anthony, K. W., Olefeldt, D., Schuur, E. A. G., Grosse, G., Kuhry, P., Hugelius, G., Koven, C., Lawrence, D. M., Gibson, C., Sannel, A. B. K., and McGuire, A. D.: Carbon release through abrupt permafrost thaw. Nature Geoscience, 13 (138):138–143. Doi:10.1038/s41561-019-0526-0, 2020.

van Bellen, S., Garneau, M., and Booth, R.K.,: Holocene carbon accumulation rates from three ombrotrophic peatlands in boreal Quebec, Canada: impact of climate-driven ecohydrological change. Holocene 21, 1217e1231, 2011.

van Everdingen, R.: Multi-Language Glossary of Permafrost and Related Ground-Ice Terms, revised May 2005. National Snow and Ice Data Center/World Data Center for Glaciology, Boulder, CO, http://nsidc.org/fgdc/glossary/, 1998.

Vitt, D. H., Halsey, L. A., and Zoltai, S. C.: The changing landscape of Canada's western boreal forest: the current dynamics of permafrost. Can. J. For. Res. 30: 283–287, 2000a.

Vitt, D. H., Halsey, L. A., Bauer, I. E., and Campbell, C.: Spatial and temporal trends in carbon storage of peatlands of continental Western Canada through the Holocene. Canadian Journal of Earth Science 37:683–693, 2000b.

Voldoire, A., Sanchez-Gomez, E., Salas y Mélia, D., Decharme, B., Cassou, C., Sénési, S., Valcke, S., Beau, I., Alias, A., Chevallier, M., Déqué, M., Deshayes, J., Douville, H., Fernandez, E., Madec, G., Maisonnave, E., Moine, M.-P., Planton, S., Saint-Martin, D., Szopa, S., Tyteca, S., Alkama, R., Belamari, S., Braun, A., Coquart, L., and Chauvin, F.: The CNRM-CM5.1 global climate model: description and basic evaluation. Climate Dynamics, 40(9): 2091-2121, DOI:10.1007/s00382-011-1259-y, 2011.

Walter Anthony, K. M., Schneider von Deimling, T., Nitze, I., Frolking, S., Emond, A., Daanen, R., Anthony, P., Lindgren, P., Jones, B., and Grosse, G.: 21st-century modeled permafrost carbon emissions accelerated by abrupt thaw beneath lakes. Nat. Commun. 9, 3262, 2018.

Watanabe, S., Hajima, T., Sudo, K., Nagashima, T., Takemura, T., Okajima, H., Nozawa, T., Kawase, H., Abe, M., Yokohata, T., and Ise, T.: MIROC-ESM 2010: model description and basic results of CMIP 5-20 c 3 m experiments. Geosci. Mod. Dev,. 4, 845-872, 2011, 2010.

Willeit, M., and Ganopolski, A.: Coupled Northern Hemisphere permafrost–ice-sheet evolution over the last glacial cycle. Clim. Past, 11, 1165–1180. doi:10.5194/cp-11-1165-2015, 2015.

Willmott, C. J., and Matsuura, K.: Terrestrial Air Temperature and Precipitation: Monthly and Annual Time Series (1950 - 1999). Available via NOAA/OAR/ESRL PSD http://climate.geog.udel.edu/~climate/html_pages/README.ghcn_ts2.html, 2001. Accessed 23 Dec 2019

Xing, W., Bao, K., Gallego-Sala, A. V., Charman, D. J., Zhang, Z., Gao, C., Lu,X., and Wang, G.: Climate controls on carbon accumulation in peatlands of Northeast China. Quaternary Science Reviews 115, 78-88, 2015.

Yokohata, T., Saito, K., ~~Takata~~Ito, A., Ohno, H., Tanaka, K., ~~Nitta, T., Satoh, Y.,~~ Hajima, T., ~~Sueyoshi, T.,~~ and Iwahana, G.~~:~~ ~~Model improvement and~~: Future projection of climate change due to permafrost ~~processes in~~degradation with a ~~global climate model. In review at~~simple numerical scheme. Progress in Earth and Planetary Science, ~~2020a~~7:56, doi:10.1186/s40645-020-00366-8, 2020.

~~Yokohata, T., Saito, K., Ito, A., Ohno, H., Tanaka, K., Hajima, T., and Iwahana, G.: Future projection of climate change due to permafrost degradation with a simple numerical scheme. In review at Progress in Earth and Planetary Science, 2020b.~~

Yoshikawa K., Bolton, W. R., Romanovsky, V. E., Fukuda, M., and Hinzman, L. D.: Impacts of wildfire on the permafrost in the boreal forests of Interior Alaska, J. Geophys. Res., 107, 8148, doi:10.1029/2001JD000438, 2002.

Yu, Z., Beilman, D. W., and Jones M. C.: Sensitivity of Northern Peatland Carbon Dynamics to Holocene Climate Change. Geophysical Monograph Series 184. 55-69. doi:10.1029/2008GM000822, 2009.

Yu, Z., Vitt, D. H., Campbell, I. D., and Apps, M. J: Understanding Holocene peat accumulation pattern of continental fens in western Canada. Canadian Journal of Botany 81:267–282. 2003.

Yu, Z., Loisel, J., Brosseau, D. P., Beilman, D. W., and Hunt, S. J.: Global peatland dymanics since the Last Glacial Maximum. GRL 37, L13402, doi:10.1029/2010GL043584, 2010.

Yu, Z.: Northern peatland carbon stocks and dynamics: a review. Biogeosciences, 9, 4071-4085, doi: 10.5194/bg-9-4071-2012, 2012.

Yukimoto, S., Adachi, Y., Hosaka, M., Sakami, T., Yoshimura, H., Hirabara, M., Tanaka, T. Y., Shindo, E., Tsujino, H., Deushi, M., and Mizuta, R.: A new global climate model of the Meteorological Research Institute: MRI-CGCM3 model description and basic performance. Journ. Met. Soc. Japan, 90A, 23-64, 2012.